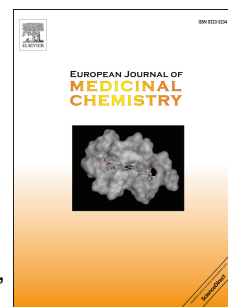# Accepted Manuscript

Design, synthesis and pharmacological evaluation of a novel mTOR-targeted anti-EV71 agent

Tianlong Hao, Yuexiang Li, Shiyong Fan, Wei Li, Shixu Wang, Song Li, Ruiyuan Cao, Wu Zhong

Please cite this article as: T. Hao, Y. Li, S. Fan, W. Li, S. Wang, S. Li, R. Cao, W. Zhong, Design, synthesis and pharmacological evaluation of a novel mTOR-targeted anti-EV71 agent, *European Journal of Medicinal Chemistry* (2019), doi: https://doi.org/10.1016/j.ejmech.2019.04.048.

# Design, synthesis and pharmacological evaluation of a novel mTOR-targeted anti-EV71 agent

Tianlong Hao[a], Yuexiang Li[a], Shiyong Fan[a], Wei Li[a], Shixu Wang[a], Song Li[a], Ruiyuan Cao[*], Wu Zhong[*]

[a] National Engineering Research Center for the Emergency Drug, Beijing Institute of Pharmacology and Toxicology, Beijing 100850, PR China

[*] Corresponding author

Wu Zhong: National Engineering Research Center for the Emergency Drug, Beijing Institute of Pharmacology and Toxicology, China; E-mail: zhongwu@bmi.ac.cn

Ruiyuan Cao: National Engineering Research Center for the Emergency Drug, Beijing Institute of Pharmacology and Toxicology, China; E-mail: 21cc@163.com

we discovered a novel anti-EV71 target—mTOR for the first time, and optimized the structure of a potent anti-EV71 inhibitor, Torin2, to obtain potent activity and better water solubility anti-EV71 agents.



Torin2
Anti-EV71 activity:
$IC_{50}$=0.01μM
Water solubility:
C=1.29μg/ml

Compound 11e
Anti-EV71 activity:
$IC_{50}$=0.027μM
Water solubility:
C=0.39μg/ml

Compound 11m
Anti-EV71 activity:
$IC_{50}$=0.09μM
Water solubility:
C=18.64μg/ml

VAL2240

LYS2187

# Design, synthesis and pharmacological evaluation of a novel mTOR-targeted anti-EV71 agent

Tianlong Hao[a], Yuexiang Li[a], Shiyong Fan[a], Wei Li[a], Shixu Wang[a], Song Li[a], Ruiyuan Cao[a,*], Wu Zhong [a,*]
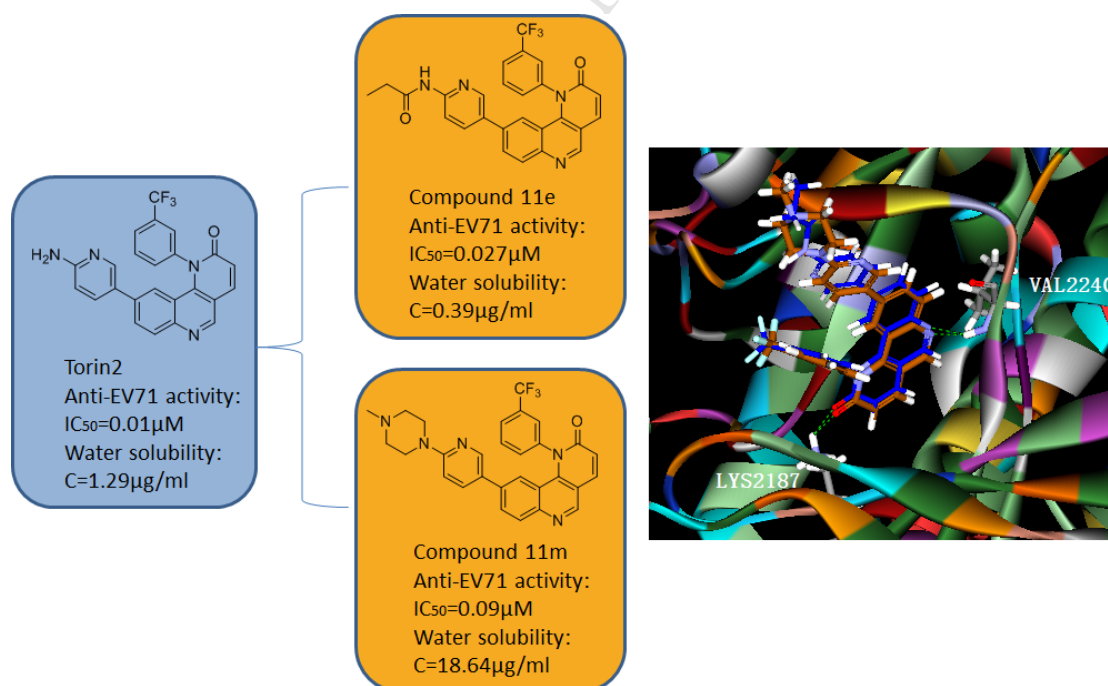
[a] National Engineering Research Center for the Emergency Drug, Beijing Institute of Pharmacology and Toxicology, Beijing 100850, PR China

[*] Corresponding author

Wu Zhong: National Engineering Research Center for the Emergency Drug, Beijing Institute of Pharmacology and Toxicology, China; E-mail: zhongwu@bmi.ac.cn

Ruiyuan Cao: National Engineering Research Center for the Emergency Drug, Beijing Institute of Pharmacology and Toxicology, China; E-mail: 21cc@163.com

## ABSTRACT

Due to the limitations of existing anti-EV71 targets, we have been eager to discover a new anti-EV71 agent based on mTOR (the mammalian target of rapamycin), which is an important target for finding antiviral agents based on host cells. Torin2 is a second-generation ATP competitive mTOR kinase inhibitor ($IC_{50}$=0.25 nM). Our research team tested the anti-EV71 activity of Torin2 *in vitro* for the first time. The result showed that Torin2 had significant anti-EV71 activity ($IC_{50}$=0.01 μM). In this study, thirty novel Torin2 derivatives were synthesized and evaluated for anti-EV71 activity. Among them, **11a**, **11b**, **11d**, **11e** and **11m** displayed similar activity to Torin2. **11e** displayed the most potent activity, with an $IC_{50}$ value of 0.027 μM, which was closest to Torin2, and displayed potent mTOR kinase inhibitory activity. A molecular modeling study showed that **11e** interacted with Val2240 and Lys2187 via hydrogen bonds and had a good match with the receptor. Additionally, a mechanism study showed that most of the compounds had significant inhibition for the mTOR pathway substrates p70S6K and Akt. The water solubility test of compounds with potent activity revealed that **11a** and **11m** were improved by approximately 5-15-fold compared to Torin2. These data suggest that **11a** and **11m** may be potential candidates for anti-EV71 treatment.

**Keywords:** mTOR; anti-EV71 Inhibitor.

## 1. Introduction

Hand-foot-and-mouth disease (HFMD) is an infectious disease caused by a variety of enteroviruses (EVs) that can be transmitted by direct contact with the gastrointestinal and respiratory systems. According to WHO statistics, a wide range of HFMD epidemics have been reported in various regions of the Western Pacific since 2010 [1, 2].

Enterovirus 71 (EV71) is the main pathogen that causes HFMD. At present, there are no effective antiviral drugs and preventive vaccines against EV71, and most of them are still in the preclinical research stage. The idea of EV71 antiviral therapy is mainly divided into two aspects. On the one hand, it directly targets the EV71 infection process, and the targets are mainly EV71 RNA-dependent RNA polymerase, VP1, and nonstructural proteins (2A, 2B, 2C, 3A, 3C and 3D). There are also some agents that block the replication process of the virus by cutting off the EV71 replication-related signaling pathways, including small molecule agents, natural products, and nucleotide therapy, but most of them lack a rigorous clinical trial basis, and the mechanism and effect need to be further clarified. Additionally, the long-term effects of certain drugs may also trigger viral resistance mutations [3-11].

Due to the limitations of existing anti-EV71 virus targets, it is of particular importance to find new targets for high-efficiency and low-toxicity against EV71. The mammalian target of rapamycin (mTOR) is a highly conserved serine/threonine protein kinase that belongs to the phosphoinositide 3-kinase (PI3K)-related protein kinase (PIKK) family [12, 13]. mTOR is a key element in the PI3K/Akt/mTOR signaling pathway that controls cell growth in response to energy, nutrients, growth factors and other environmental cues [14]. It exists in two functionally distinct protein complexes, mTORC1 and mTORC2. The mTORC1 complex is composed of Raptor, LST8, PRAS40 and Deptor, and is responsible for regulated protein synthesis through phosphorylation of S6K1 and 4EBP1. The mTORC2 complex consists of Rictor, LST8, SIN1, Deptor, and Protor, and regulates cell proliferation and survival through phosphorylation of Akt/PKB. After the virus attaches and enters the host cell, it activates the PI3K/Akt/mTOR signaling pathway, upregulates the phosphorylation level of downstream functional factors S6K1 and 4EBP1 of mTOR, reduces the host cell apoptosis caused by a viral infection, and makes the virus continue to infect the cell [15]. A manuscript describing the mechanism of action studies is in preparation and will be published elsewhere.

In recent years, studies to inhibit viruses by inhibiting mTOR of host cells have been widely reported [16-28]. We collected the existing mTOR inhibitors in the preclinical research stage and tested their activities against the EV71 *in vitro* [29-41]. Our experimental data showed that Torin2, which is a mTORC1 and mTORC2 dual inhibitor [42], exhibits potent activity against EV71 with an $IC_{50}$ of 0.01 μM. Although Torin2 showed high activity and suitable bioavailability (F=51%), its water solubility is poor. We measured its solubility in water as 1.29 μg/ml which is almost insoluble according to Ch.P. (Pharmacopoeia of The People's Republic of China). Moreover, as water solubility is an important physicochemical property affecting the absorption of oral drugs, we considered to improve the water solubility of Torin2 through structural modification while maintaining high activity. To overcome these deficiencies, we initiated a medicinal chemistry campaign that resulted in the identification of a highly potent anti-EV71 agent targeting mTOR.

## 2. Results and Discussion

### 2.1. Chemistry

Based on the early studies [42, 43] and the analysis of Torin2 and mTOR protein cocrystallization, we optimized the structure of Torin2 and obtained the preliminary structural formula (**1'**) of the designed compounds. The heterocycle A and B was an essential part of the activity, and it needed to contain an electron-rich structure to form a hydrogen bond with the amino acid residue; a quinoline ring was selected as the core structure. Ring C was mainly used to maintain its pharmacokinetic properties, and a 3-trifluoromethylphenyl was selected. Part D filled the hydrophobic pocket region of the acceptor, primarily a five or six-membered aromatic heterocyclic ring or a flexible long-chain substitution. Therefore, we decided to retain the quinoline ring structure of Part A and B and the 3-trifluoromethylphenyl structure of Part C. We redesigned Part D and Part E and investigated its effect on the structure-activity relationship. We designed series 1, 2 and 3 compounds and investigated the effects of the lactam structure, the oxazolone structure and the ketene side chain structure of Part E on the activity. For Part D, we chose aromatic rings, aromatic heterocycles, spiro rings, and chain substituents to investigate the effect of different conjugated systems and different spatially oriented substitutions on activity.

**Figure 1**

3

6-bromo-4-((3-(trifluoromethyl)phenyl)amino)quinoline-3-carbaldehyde (**2**) was synthesized according to a method previously reported in the literature [42]. The Horner-Wadsworth -Emmons olefination reaction of **2** with ethyl 2-(diethoxyphosphoryl) acetate in the presence of potassium carbonate provided the intermediate **3** [44]. The Suzuki coupling reaction of intermediate **3** with different boronic esters in the presence of Pd(PPh$_3$)$_4$ and potassium carbonate provided the compounds **4a**-**4b** [42]. Intermediate **3** reacted with different substituted aromatic amines via a coupling reaction to afford compounds **4c**-**4d** [45]. (**Scheme 1**).

**Scheme 1**

The oxidation reaction of **2** with MCPBA in the presence of potassium carbonate provided the intermediate **5**, which was treated with NaOH (1N) to give intermediate **6**. Then, intermediate **6** reacted with *N*,*N'*-Carbonyldiimidazole via a condensation reaction to afford intermediate **7**. The Suzuki coupling reaction of intermediate **7** with different boronic esters in the presence of Pd(PPh$_3$)$_4$ and potassium carbonate provided the compounds **8a**-**8c** [46]. Intermediate **7** reacted with different enamides or olefins via a coupling reaction to afford compounds **8d**-**8f** [47]. (**Scheme 2**).

**Scheme 2**

Compound **2** reacted with 1-(triphenylphosphoranylidene)propan-2-one via a coupling reaction to afford intermediate **9**. The Suzuki coupling reaction of intermediate **9** with different boronic esters in the presence of Pd(PPh$_3$)$_4$ and potassium carbonate provided the compounds **10a**-**10e** [48]. (**Scheme 3**).

**Scheme 3**

Finally, considering the excellent anti-EV71 activity of compound **4b**, a series of analogues, **11a**-**11o**, were synthesized with different substitutions at the R$_4$, R$_5$ and R$_6$-position via different substituted pyridyl derivatives, such as alkyl, methoxy, fluoro, alkylamide, arylamide-substituted

4

pyridine, other ring-substituted pyridine and quinolone to improve activity and pharmacokinetic properties [42-44]. (**Scheme 4**).

**Scheme 4**

## 2.2. Biology

### 2.2.1. Anti-EV71 Activities and the SARs

Starting from the lead-compound Torin2, **4a**-**4d, 8a**-**8f,** and **10a**-**10e** were synthesized, and their anti-EV71 activities were evaluated in RD cell lines. The results listed in **Table 1** indicated that compared to the compounds of series 2 and series 3, the series 1 compounds generally have certain antiviral activities, of which compound **4b** displayed closer anti-EV71 activity to Torin2.

**Table 1**

To search for potential compounds that display better activity and pharmacokinetic properties, the reactions of intermediate **3** with different substituted pyridine derivatives were performed to obtain compounds **11a**-**11o**. In this series of analogues, we mainly investigated the effects of the location, size, electronegativity of different substitutions on pyridyl, and obtained some obvious SARs. The results listed in **Table 2** indicated that the position and size of the substitution on pyridine moiety was crucial for anti-EV71 activity.

Compound **11a**, which contained -F at the C-2 ($R_4$) position of the pyridine moiety displayed some higher anti-EV71 activity compared to compound **11b**, which contains -F at the C-6 ($R_6$) position. Compound **11c**, which contained -$OCH_3$ at the C-2 ($R_4$) position, lost activity ($IC_{50} >$ 200 μM). Moving the -$OCH_3$ group from the C-2 position to the C-6 position significantly increased the anti-EV71 activity (Compound **11d**: $IC_{50}$ values of 0.04 μM). Therefore, when the substitution was an electron-donating group and located at the C-6 position, it displayed better activity.

On the other hand, as shown in compound **11e**-**11o**, when the C-6 ($R_6$) position was substituted by a N derivative, the anti-EV71 activity of the compound can be maintained. Compound **11e**, **11f** and **11h** were all substituted by a linear amide group. Among them, the

propionamide-substituted compound **11e** displayed the best activity (IC$_{50}$ values of 0.027 μM) close to the reference compound Torin2, but the activity gradually decreased with extension of the length of the substitution. When a linear substitution (compound **11f**) is replaced by a branched substitution (compound **11g**), the activity significantly decreased. The activity of compound **11i**, which was obtained by replacing the terminal substitution with a phenyl group, was lower than that of compound **11e**. Therefore, the SARs in the amide substituted compound was that the chain substituted compounds were superior to the aromatic ring substituted compounds. The length of the chain substitution had a significant influence on the activity, the shorter the substitution length was, the better the activity.

The compound **11k** substituted with an aryloxyamide displayed moderate activity, and when the substitution was replaced by a benzyloxyamide (compound **11l**), the activity was greatly lower. Similarly, when replaced with a t-butoxyamide group, the activity of compound **11j** decreased.

If R$_6$ was a heterocyclic substitution, the compound **11m,** having a piperazine substitution, displayed moderate activity, and if the piperazine of the compound **11m** was replaced by a morphine (compound **11n**) or a pyrrolidine (compound **11o**), the activity would be significantly reduced. Therefore, the SARs of the cyclic substituted compound was that the activity of the six-membered ring-substituted compound was superior to that of the five-membered ring-substituted compound, and the activity of the double-N-ring-substituted compound was superior to that of the single-N-ring-substituted compound. The SARs of all the synthesized compounds are summarized in **Figure 2**.

**Table 2**

**Figure 2**

### 2.2.2. *In vitro* **mTOR Kinase Inhibitory Activity**

To elucidate whether the synthesized compounds target the mTOR kinase, the *in vitro* mTOR kinase inhibitory activities of **8a**, **10a** and **11e,** which were the representative compounds of the respective series, were evaluated in regard to their relatively better anti-EV71 activities among

all the tested compounds. The inhibitory concentrations that inhibited the mTOR kinase by 50% ($IC_{50}$) of compounds **8a**, **10a**, and **11e** were 256.80, 7766, and 29.24 nM, respectively. **Figure 3.**

**Figure 3**

### 2.2.3. Molecular Modeling Study

Compound **11e** displayed the best anti-EV71 activity and effective mTOR kinase inhibition in the initial screening, and we then selected it as the optimized compound for the following studies. To explore the binding modes of target compounds with the ATP-binding site of mTOR, molecular docking simulation studies were carried out by using the Libdock module of the Discovery Studio 2.5. When docking compound **11e**, **Figure 4**A shows that compound **11e** could be docked in the ATP-binding site in a similar conformation to that of the reference compound Torin2 in the crystal structure (PDB ID code: 4JSV). Since numerous studies have suggested that the interaction to the hinge region is crucial to mTOR inhibitory activity, the interaction with Val2240 is essential to many kinds of mTOR inhibitors [49-56]. Compound **11e** and Torin2 could overlap in the position of the ring structure. The nitrogen atom on the quinoline group and the oxygen atom on the carbonyl group of **11e** and Torin2, respectively, bond to Val2240 and Lys2187 via a hydrogen bond. Moreover, the structure of quinoline in **11e** and Torin2 is fixed on the central hydrophobic region of the ATP-binding site with a π-π conjugation effect with Trp2239. To elucidate the SARs that were concluded from the anti-EV71 activities above, molecular docking was also performed to study the binding mode of some representative compounds. Comparing the docking results of **11e** and **8a** (the representative compounds of series 2), compound **8a** lost the hydrogen bond interaction with the Lys2187 (**Figure 4**B), which played a vital role in binding with the ATP-binding site. Similarly, In comparison with **11e**, the decrease in the anti-EV71 activity of **10a** might be due to the loss of the hydrogen bond with Lys2187 (**Figure 4**C). Moreover, the structure of **10a** was reversed, and the interaction between the ketene side chain and the hydrophobic cavity was decreased compared to **11e**. In comparison with **11e**, compounds **11d**, **11h** and **11m** formed the same hydrogen bonds with Val2240 and Lys2187 in the ATP-binding site. This might explain why their activity was close to **11e**. However, due to the increase in the size of the long chain substitution of the compound **11h** (**Figure 4**E) and the piperazine substitution of the compound **11m** (**Figure 4**F), it was more

easily exposed to the solvent environment. On the other hand, compared with **11e**, we found the activity decline of the -OCH$_3$ substituted **11d** (**Figure 4**D) because the -OCH$_3$ substitution was not enough to occupy the hydrophobic cavity. Therefore, the size of the substitution was critical for activity.

**Figure 4**

### 2.2.4. Cell-based Enzyme Inhibition Assay

As reported in the references, ATP competitive inhibitors of mTOR inhibit both mTORC1 and mTORC2 complexes and have a greater inhibitory function against mTORC2 than mTORC1 single inhibitors [57-59]. We performed a mTORC1 and mTORC2 cell-based assay to evaluate inhibitory activity and the molecular mechanism of the synthesized compounds in RD cells. mTORC1 activates the activity of P70S6K1 by phosphorylating the Thr389 site of P70S6K1, mTORC2 activates Akt by phosphorylating the Ser473 site of Akt. Therefore, the degree of phosphorylation of the Thr389 site of P70S6K1 and the Ser473 site of Akt in the test cells can be detected to reflect the inhibition of intracellular mTORC1 and mTORC2 by the compound. In this study, both p70 and Akt phosphorylation levels were evaluated in the mTORC1 and mTORC2 pathways of the RD cell line with the treatment of 20 μM of the compounds in the medium containing 167 nM of insulin for 2 h. Meanwhile, there were decreasing expression levels of p70 phosphorylation due to the Rapamycin (a mTORC1 single inhibitor) treatment under the same assay condition. The results are shown in **Figure 5**. Based on these observations, we concluded that compounds **4a, 4b, 4c, 4d, 11a, 11b, 11d, 11e, 11f, 11g, 11h, 11i, 11j, 11k, 11l, 11m, 11n,** and **11o** could downregulate p70 phosphorylation expression levels. Compounds **4b, 4c, 4d, 11a, 11b, 11d, 11e, 11f, 11g, 11h, 11i, 11j, 11k, 11l, 11n,** and **11o** significantly decreased the expression levels of phosphorylated Akt. The assay results showed that most series 3 compounds had dual inhibition of the mTORC1 and mTORC2 pathways. However, compounds **8a** and **8d** of series 2 and compound **10a** of series 3 can inhibit neither mTORC1 nor mTORC2, which was consistent with the lower mTOR kinase inhibitory activity of compounds **8a** and **10a**.

**Figure 5**

### 2.2.4. Absorption Properties and Water Solubility

As the poor absorption properties of Torin2 are the main factors that restrict its druggability, the absorption properties of compounds **11a**, **11b**, **11d**, **11e**, and **11m,** which displayed potent activity, attracted our attention and were predicted using software ADMET Predictor version 8.5 (Simulations Plus Inc., Lancaster, CA, USA) [60]. The computer simulation results listed in **Table 3** revealed that the absorption properties of compounds **11a**, **11b**, **11d**, **11e** and **11m** were all in a reasonable range, which suggested that **11a**, **11b**, **11d**, **11e** and **11m** were excellent candidates for potential anti-EV71 agents.

**Table 3**

As the poor absorption of Torin2 may be due to the limited water solubility [42]. We measured the water solubility of **11a**, **11b**, **11d**, **11e** and **11m**. The results are listed in **Table 4**. The water solubility of **11b**, **11d** and **11e** were worse than Torin2. However, compared to Torin2, the water solubility of **11a** was improved by approximately 5-fold, of which **11m** was improved by approximately 15-fold, which suggested that **11a** and **11m** may display better absorption properties than Torin2 for potential anti-EV71 agents and have the potential to become candidates with good druggability.

**Table 4**

### 3. Conclusions

Due to the limitations of existing anti-EV71 targets, it is especially urgent to find new safe and efficient targets. The past few years witnessed the rapid development of the novel mTOR inhibitors as antiviral agents. Torin2 analogues are one of the most representative classes displaying mTOR kinase inhibition. On the basis of our previous work, we focused the study on the Torin2 derivatives derived from different core structures, including six-membered ring compounds (series 1), five-membered ring compounds (series 2) and open-loop compounds (series 3). The comprehensive and detailed SARs we acquired might provide some information for the design and synthesis of new anti-EV71 agents. In the present work, we evaluated the

inhibitory activities of the newly synthesized 30 compounds toward EV71 in RD cell lines. Notably, compound **11e** displayed the most potent *in vitro* anti-EV71 activity. To elucidate the SARs, we conducted molecular docking studies on representative compounds. The docking results displayed that compound **11e** showed the best anti-EV71 activity and effective mTOR kinase inhibition in the initial screening and interacted with Val2240 and Lys2187 via the hydrogen bond, with a good match with the receptor. We therefore conclude that the necessary hydrogen bonding and appropriate substitution size promoted the activity. To evaluate the molecular mechanism of the compounds of the examples in RD cells, we performed mTORC1 and mTORC2 cell-based assays. Most compounds had dual inhibition of the mTORC1 and mTORC2 pathways. As water solubility is an important physicochemical property affecting the absorption of oral drugs, and water solubility is the main factor hindering Torin2's druggability, we predicted the absorption properties and measured the water solubility of synthesized compounds with potent activity. The results revealed that the absorption properties of the compounds were all in a reasonable range, and compared to Torin2, the water solubility of **11a** and **11m,** which displayed similar anti-EV71 activity to Torin2, was improved by approximately 5-15-fold. All together, we developed anti-EV71 agents based on the mTOR target for the first time, and found some potential candidates with better water solubility and potent activity. Research on these compounds is ongoing, and further efforts are in process to find excellent candidates for potential anti-EV71 agents.

## 4. Experiment Section

### 4.1. Chemistry

All reagents and solvents were used as received from commercial sources. ^{1}H-NMR and ^{13}C-NMR spectra were recorded at 400 MHz and 100 MHz on a JNM-ECA-400 instrument (JEOL Ltd., Tokyo, Japan) in DMSO-D$_6$. Chemical shifts are expressed in δ (ppm), with tetramethylsilane (TMS) functioning as the internal reference. Coupling constants (*J*) were expressed in Hz. High-resolution mass spectra were obtained using a TOF G6230A LC/MS (Agilent Technologies, New York, NY, USA) with an ESI source. Melting points were determined using an RY-1 apparatus (Yutong Company, Shanghai, China). Reagents and solvents were commercially available without further purification. The ^{1}H-NMR, ^{13}C-NMR and HRMS spectra of the compounds in this article can be found in Supporting Information.

**General Procedure for the Preparation of 4a-4d, 8a-8f, 10a-10e and 11a-11o.**

*9-bromo-1-(3-(trifluoromethyl)phenyl)benzo[h][1,6]naphthyridin-2(1H)-one (3)* Intermediate **2** was synthesized according to a method previously reported in the literature [42]. To a solution of compound **2** (3.95 g, 10 mmol), $K_2CO_3$ (4.15 g, 30 mmol) and ethyl 2-(diethoxyphosphoryl) acetate (6.73 g, 30 mmol) in dry EtOH was added. The resulting mixture was heated to 100°C for 12 h before cooling to room temperature. Upon removal of the solvents under a vacuum, the residue was diluted with water followed by extraction with EtOAc. Purification of the residue by ISCO (hexanes/EtOAc 5:1) provided compound **3**, a yellow solid. (2.87 g, 68.6% yield). ^{1}H NMR (400 MHz, DMSO-D$_6$) δ(ppm): 9.19 (s, 1H), 8.34 (d, *J* = 9.5 Hz, 1H), 8.07 (dd, *J* = 9.3, 8.8 Hz, 2H), 7.95 (dd, *J* = 17.2, 8.4 Hz, 2H), 7.86 – 7.79 (m, 2H), 6.98 (d, *J* = 9.5 Hz, 1H), 6.58 (d, *J* = 2.0 Hz, 1H). ^{13}C NMR (101 MHz, DMSO-D$_6$) δ(ppm): 162.92, 152.05, 148.04, 148.02, 141.58, 141.26, 140.64, 134.03, 133.15, 132.87, 132.02, 131.70, 131.37, 127.70, 126.83, 122.86, 119.21, 118.84, 114.21. HR-MS (ESI) m/z: calcd. for $C_{19}H_{10}BrF_3N_2O$ [M + H]$^+$: 418.9929, found: 419.0001. Mp 192–195 °C.

*9-(2-oxoindolin-5-yl)-1-(3-(trifluoromethyl)phenyl)benzo[h][1,6]naphthyridin-2(1H)-one (4a)* To a solution of compound **3** (4.18 g, 10 mmol) in 1,4-dioxane at room temperature, we subsequently added Pd(PPh$_3$)$_4$ (1.16 g, 1 mmol), $K_2CO_3$ (2.76 g, 20 mmol), and (2-oxoindolin-5-yl)boronic acid (2.12 g, 12 mmol). After degassing, the resulting mixture was heated to 80 °C for 4 h before cooling to room temperature. The solution was extracted with EtOAc. The organic layer was washed with water and brine, dried (MgSO$_4$), filtered, and evaporated to dryness as a yellow solid. (3.89 g, 82.6% yield) ^{1}H NMR (400 MHz, DMSO-D$_6$) δ(ppm): 10.53 (s, 1H), 9.15 (s, 1H), 8.34 (d, *J* = 9.5 Hz, 1H), 8.13 (dd, *J* = 25.1, 8.2 Hz, 3H), 8.05 – 7.87 (m, 2H), 7.83 (d, *J* = 7.9 Hz, 1H), 7.15 (d, *J* = 7.7 Hz, 1H), 6.98 (dd, *J* = 22.7, 5.5 Hz, 2H), 6.64 – 6.47 (m, 2H), 3.51 (s, 2H). ^{13}C NMR (101 MHz, DMSO-D$_6$) δ(ppm): 177.18, 163.10, 151.41, 148.69, 144.94, 142.53, 141.91, 140.81, 139.01, 137.60, 133.90, 132.15, 131.99, 131.69, 131.42, 129.27, 127.01, 126.31, 125.01, 123.10, 122.90, 122.28, 120.36, 117.81, 114.09, 107.60, 36.04. HR-MS (ESI) m/z: calcd. for $C_{27}H_{16}F_3N_3O_2$ [M + H]$^+$: 472.1195, found: 472.1268. Mp 281–282 °C.

*9-(6-(dimethylamino)pyridin-3-yl)-1-(3-(trifluoromethyl)phenyl)benzo[h][1,6]naphthyridin-2(1H)-one (4b)* The title compound was obtained similarly to **4a**. The boronic acid was replaced with (6-(dimethylamino)pyridin-3-yl)boronic acid. (yellow solid, yield: 82.4%). ^{1}H NMR (400 MHz, DMSO-D$_6$) δ(ppm): 9.10 (s, 1H), 8.32 (d, *J* = 9.5 Hz, 1H), 8.13 (s, 1H), 8.06 (dd, *J* = 8.1,

3.5 Hz, 2H), 8.00 (d, $J$ = 2.4 Hz, 1H), 7.96 (dd, $J$ = 8.7, 1.8 Hz, 1H), 7.90 (t, $J$ = 7.9 Hz, 1H), 7.80 (d, $J$ = 8.0 Hz, 1H), 7.06 (dd, $J$ = 8.9, 2.6 Hz, 1H), 6.93 (t, $J$ = 5.6 Hz, 2H), 6.57 (d, $J$ = 8.9 Hz, 1H), 3.05 (s, 6H). $^{13}$C NMR (101 MHz, DMSO-D$_6$) δ(ppm): 163.12, 158.83, 150.85, 148.29, 146.25, 142.17, 141.98, 140.82, 135.40, 135.28, 133.89, 132.03, 131.59, 131.39, 131.26, 128.31, 127.14, 126.64, 122.30, 122.18, 121.11, 117.99, 114.08, 105.82, 38.10. HR-MS (ESI) m/z: calcd. for C$_{26}$H$_{19}$F$_3$N$_4$O [M + H]$^+$: 461.1511, found: 461.1585. Mp 220–222 °C.

*General procedure for the preparation of 9-((3-aminophenyl)amino)-1-(3-(trifluoromethyl) phenyl)benzo[h][1,6]naphthyridin-2(1H)-one(4c)* To a solution of compound **3** (4.18 g, 10 mmol) in 1,4-dioxane at room temperature, we subsequently added Pd(dba)$_3$ (0.23 g, 0.25 mmol), CsCO$_3$ (4.88 g, 15 mmol), 1,3-phenylenediamineand (1.62 g, 15 mmol) and 4,5-Bis (diphenylphosphino)-9,9-dimethylxanthene (0.14 g, 0.25 mmol). The resulting mixture was heated to 100 °C for 2 h under a N$_2$ atmosphere. The solution was extracted with EtOAc. The organic layer was washed with water and brine, dried (MgSO$_4$), filtered, and evaporated to dryness as a yellow solid. (3.52 g, 78.8% yield). $^1$H NMR (400 MHz, DMSO-D$_6$) δ(ppm): 8.85 (s, 1H), 8.22 (d, $J$ = 9.5 Hz, 1H), 7.94 (s, 1H), 7.86 (d, $J$ = 9.0 Hz, 1H), 7.78 (d, $J$ = 8.1 Hz, 1H), 7.63 (dd, $J$ = 14.4, 6.4 Hz, 2H), 7.53 (d, $J$ = 7.9 Hz, 1H), 7.29 (dd, $J$ = 9.0, 2.4 Hz, 1H), 6.89 – 6.80 (m, 2H), 6.43 (d, $J$ = 2.3 Hz, 1H), 6.21 (dd, $J$ = 7.9, 1.3 Hz, 1H), 6.07 (t, $J$ = 2.0 Hz, 1H), 5.87 – 5.75 (m, 1H), 5.15 (s, 2H). $^{13}$C NMR (101 MHz, DMSO-D$_6$) δ(ppm): 163.08, 149.72, 147.18, 144.29, 142.66, 142.42, 140.96, 140.81, 140.76, 133.62, 131.57, 131.43, 130.78, 130.47, 130.08, 125.39, 123.80, 122.80, 121.75, 118.98, 114.25, 108.69, 107.17, 105.64, 105.16. HR-MS (ESI) m/z: calcd. for C$_{25}$H$_{17}$F$_3$N$_4$O [M + H]$^+$: 447.1354, found: 447.1427. Mp 217–218 °C.

*9-((6-aminopyridin-2-yl)amino)-1-(3-(trifluoromethyl)phenyl)benzo[h][1,6]naphthyridin-2(1 H)-one (4d)* The title compound was obtained similarly to **4c**. 1,3-phenylenediamineand was replaced with pyridine-2,6-diamine. (yellow solid, yield: 81.3%). $^1$H NMR (400 MHz, DMSO-D$_6$) δ(ppm): 8.91 (s, 1H), 8.50 (s, 1H), 8.25 (d, $J$ = 9.5 Hz, 1H), 7.95 (d, $J$ = 8.0 Hz, 1H), 7.87 (d, $J$ = 9.0 Hz, 1H), 7.66 (dt, $J$ = 13.4, 7.8 Hz, 3H), 7.52 (dd, $J$ = 9.0, 2.3 Hz, 1H), 7.22 – 7.11 (m, 2H), 6.86 (d, $J$ = 9.4 Hz, 1H), 5.91 (d, $J$ = 7.9 Hz, 1H), 5.71 (t, $J$ = 14.5 Hz, 3H). $^{13}$C NMR (101 MHz, DMSO-D$_6$) δ(ppm): 163.02, 148.31, 141.68, 141.18, 140.71, 134.17, 131.40, 130.91, 130.87, 130.58, 125.83, 125.80, 125.66, 125.63, 125.51, 125.11, 122.80, 122.05, 120.74, 118.47, 114.24, 114.22, 100.00, 97.26. HR-MS (ESI) m/z: calcd. for C$_{24}$H$_{16}$F$_3$N$_5$O [M + H]$^+$: 448.1307, found: 448.1380. Mp 259–261 °C.

*6-bromo-4-((3-(trifluoromethyl)phenyl)amino)quinolin-3-yl formate (5)* To a solution of compound **2** (3.95 g, 10 mmol) in DCM at room temperature, we added 3-chloroperoxybenzoic acid (3.45 g, 20 mmol). The resulting mixture was stirred at room temperature for 1 h. Upon removal of the solvents, the residue was subjected to column purification (DCM/MeOH 10:1) to furnish the desired compound **5** as a yellow solid. (3.25 g, 79.2% yield). $^1$H NMR (400 MHz, DMSO-D$_6$)δ(ppm): 9.07 (s, 1H), 8.85 (s, 1H), 8.03 – 7.87 (m, 3H), 7.79 – 7.75 (m, 1H), 7.70 (ddd, $J$ = 4.5, 2.1, 1.0 Hz, 1H), 7.60 – 7.52 (m, 2H), 7.40 (dd, $J$ = 23.0, 6.1 Hz, 1H). $^{13}$C NMR (101 MHz, DMSO-D$_6$) δ(ppm): 166.63, 163.07, 148.84, 146.18, 142.35, 141.86, 133.26, 132.09, 131.44, 131.20, 130.20, 129.37, 128.46, 125.23, 124.19, 123.54, 122.24. HR-MS (ESI) m/z: calcd. for $C_{17}H_{10}BrF_3N_2O_2$ [M + H]$^+$: 410.9878, found: 410.9950. Mp 176–179 °C.

*6-bromo-4-((3-(trifluoromethyl)phenyl)amino)quinolin-3-ol (6)* A solution of compound **5** (4.10 g, 10 mmol) in NaOH (1 N) at room temperature was heated to 50 °C for 4 h. After the mixture was cooled to room temperature, a solution of AcOH (1 N) was added to neutralize the solution followed by dilution with water and extraction with EtOAc. After the organic layer was dried with Na$_2$SO$_4$, the solvents were removed and the residue was purified by ISCO (hexanes/EtOAc 5:1) to furnish compound **6** as a yellow solid. (3.27 g, 85.6% yield). $^1$H NMR (400 MHz, DMSO-D$_6$) δ(ppm): 10.47 (s, 1H), 8.68 (d, $J$ = 22.9 Hz, 2H), 8.25 – 8.14 (m, 1H), 7.93 – 7.85 (m, 1H), 7.67 (dd, $J$ = 8.9, 2.2 Hz, 1H), 7.37 (t, $J$ = 7.9 Hz, 1H), 7.07 (d, $J$ = 7.7 Hz, 1H), 6.98 (s, 1H), 6.92 – 6.83 (m, 1H). $^{13}$C NMR (101 MHz, DMSO-D$_6$) δ(ppm):145.27, 144.95, 144.83, 142.65, 131.99, 130.00, 129.71, 127.31, 126.45, 126.30, 124.90, 123.60, 120.17, 119.17, 115.00, 111.79. HR-MS (ESI) m/z: calcd. for $C_{16}H_{10}BrF_3N_2O$ [M + H]$^+$: 382.9929, found: 383.0001. Mp 184–186 °C.

*8-bromo-1-(3-(trifluoromethyl)phenyl)oxazolo[5,4-c]quinolin-2(1H)-one (7)* To a solution of compound **6** (3.82 g, 10 mmol) in dry THF at room temperature, we added *N,N′*-Carbonyldiimidazole (2.43 g, 15 mmol). The resulting mixture was stirred at room temperature for 4 h. Upon removal of the solvents, the residue was subjected to column purification (DCM/MeOH 10:1) to furnish the desired compound **7** as a yellow solid. (3.10 g, 75.9% yield). $^1$H NMR (400 MHz, DMSO-D$_6$)δ(ppm): 9.18 (s, 1H), 8.31 (d, $J$ = 1.9 Hz, 1H), 8.15 (ddd, $J$ = 8.6, 1.7, 0.6 Hz, 2H), 8.07 – 7.99 (m, 2H), 7.83 (dd, $J$ = 9.1, 2.2 Hz, 1H), 7.65 (s, 1H). $^{13}$C NMR (101 MHz, DMSO-D$_6$) δ(ppm): 153.07, 144.44, 137.15, 135.69, 135.17, 134.88,

133.47, 133.16, 132.17, 132.05, 131.92, 131.07, 127.84, 126.17, 122.60, 120.55, 116.46. HR-MS (ESI) m/z: calcd. for $C_{17}H_8BrF_3N_2O_2$ $[M + H]^+$: 408.9721, found: 408.9793. Mp 193–195 °C.

*8-(6-methylpyridin-3-yl)-1-(3-(trifluoromethyl)phenyl)oxazolo[5,4-c]quinolin-2(1H)-one   (8a)*
To a solution of compound **7** (4.08 g, 10 mol) in 1,4-dioxane at room temperature, we subsequently added Pd(PPh$_3$)$_4$ (1.16 g, 1 mmol), K$_2$CO$_3$ (2.76 g, 20 mmol), and (6-methylpyridin-3-yl)boronic acid (1.64 g, 12 mmol). After degassing, the resulting mixture was heated to 80 °C for 4 h before cooling to room temperature. The solution was extracted with EtOAc. The organic layer was washed with water and brine, dried (MgSO$_4$), filtered, and evaporated to dryness. As a yellow solid (3.59 g, 85.3% yield). $^1$H-NMR (400 MHz, DMSO-D$_6$) δ (ppm): 9.36 (s, 1H), 8.82 (d, $J$ = 2.0 Hz, 1H), 8.42 – 8.35 (m, 2H), 8.28 (ddd, $J$ = 15.9, 8.6, 4.5 Hz, 3H), 8.12 (d, $J$ = 8.0 Hz, 1H), 8.03 (t, $J$ = 7.9 Hz, 1H), 7.93 (d, $J$ = 8.4 Hz, 1H), 7.29 (d, $J$ = 1.8 Hz, 1H), 2.77 (s, 3H). $^{13}$C NMR (101 MHz, DMSO-D$_6$) δ (ppm): 154.29, 153.07, 143.94, 142.35, 140.01, 137.09, 135.01, 134.77, 133.92, 133.47, 133.21, 132.16, 131.37, 131.04, 130.01, 129.06, 128.13, 127.94, 126.13, 125.40, 119.51, 115.11, 19.81. HR-MS (ESI) m/z: calcd. for $C_{23}H_{14}F_3N_3O_2$ $[M + H]^+$: 422.1038, found: 422.1111. Mp 299–300 °C.

*8-(5-methoxypyridin-3-yl)-1-(3-(trifluoromethyl)phenyl)oxazolo[5,4-c]quinolin-2(1H)-one*
*(8b)* The title compound was obtained similarly to **8a**. The boronic acid was replaced with (5-methoxypyridin-3-yl)boronic acid. (yellow solid, yield: 83.1%). $^1$H-NMR (400 MHz, DMSO-D$_6$) δ(ppm): 9.17 (s, 1H), 8.38 (s, 1H), 8.28 (d, $J$ = 2.7 Hz, 1H), 8.22 (d, $J$ = 8.9 Hz, 2H), 8.18 – 8.11 (m, 3H), 8.01 (t, $J$ = 7.9 Hz, 1H), 7.32 – 7.29 (m, 1H), 7.15 (d, $J$ = 1.8 Hz, 1H), 3.84 (s, 3H). $^{13}$C NMR (101 MHz, DMSO-D$_6$) δ (ppm): 156.10, 153.20, 145.50, 139.82, 138.08, 137.03, 135.46, 135.28, 134.94, 133.72, 132.94, 132.12, 131.75, 131.42, 131.10, 128.13, 127.75, 126.40, 125.41, 118.26, 118.16, 115.49, 56.08. HR-MS (ESI) m/z: calcd. for $C_{23}H_{14}F_3N_3O_3$ $[M + H]^+$: 438.0987, found: 438.1060. Mp 257–258 °C.

*8-(quinolin-3-yl)-1-(3-(trifluoromethyl)phenyl)oxazolo[5,4-c]quinolin-2(1H)-one (8c)* The title compound was obtained similarly to **8a**. The boronic acid was replaced with quinolin-3-ylboronic acid. (gray solid, yield: 82.2%). $^1$H-NMR (400 MHz, DMSO-D$_6$) δ (ppm): 9.19 (s, 1H), 8.85 (d, $J$ = 2.4 Hz, 1H), 8.44 – 8.40 (m, 2H), 8.30 – 8.23 (m, 3H), 8.19 (d, $J$ = 8.0 Hz, 1H), 8.08 – 8.02 (m, 2H), 7.96 (d, $J$ = 7.3 Hz, 1H), 7.83 – 7.78 (m, 1H), 7.71 – 7.67 (m, 1H), 7.29 (s, 1H).$^{13}$C-NMR (101 MHz, DMSO-D$_6$) δ (ppm): 153.19, 148.99, 147.48, 145.45, 137.09, 135.53, 135.29, 134.94, 133.77, 132.96, 132.21, 131.94, 131.84, 131.41, 131.09, 130.70, 129.23, 128.77,

128.14, 128.03, 127.87, 127.80, 126.37, 125.47, 118.32, 115.62. HR-MS (ESI) m/z: calcd. for $C_{26}H_{14}F_3N_3O_2$ [M + H]$^+$: 458.1038, found: 458.1111. Mp 242–244 °C.

*(E)-1-(3-(2-oxo-1-(3-(trifluoromethyl)phenyl)-1,2-dihydrooxazolo[5,4-c]quinolin-8-yl)allyl)urea (8d)* To a solution of compound **7** (4.08 g, 10 mmol) in DMF at room temperature, we added Pd(OAc)$_2$ (0.45 g, 2 mmol), 1-allylurea (2.00 g, 20 mmol), Tri(o-tolyl)phosphine (1.22 g, 4 mmol) and Et$_3$N(10.12 g, 100 mmol). The resulting mixture was heated to 100 °C for 2 h under N$_2$ atmosphere. The residue was diluted with water followed by extraction with EtOAc. The organic layer was washed with water and brine, dried (MgSO$_4$), filtered, and evaporated to dryness, yellow solid (3.64g, 84.9% yield). $^1$H NMR (400 MHz, DMSO-D$_6$) δ(ppm): 9.06 (s, 1H), 8.30 (s, 1H), 8.17 – 8.09 (m, 2H), 8.05 – 7.96 (m, 2H), 7.86 (d, *J* = 9.1 Hz, 1H), 6.78 (s, 1H), 6.25 – 6.11 (m, 3H), 5.51 (s, 2H), 3.70 (t, *J* = 5.4 Hz, 2H). $^{13}$C NMR (101 MHz, DMSO-D$_6$) δ(ppm): 158.96, 153.22, 145.27, 136.96, 135.64, 135.22, 133.80, 133.40, 132.65, 132.21, 131.99, 131.07, 130.65, 128.48, 127.67, 126.85, 126.22, 117.52, 115.55, 115.17, 113.65. HR-MS (ESI) m/z: calcd. for $C_{21}H_{15}F_3N_4O_3$ [M + H]$^+$: 429.1096, found: 429.1169. Mp 158–160 °C.

*(E)-4-(2-oxo-1-(3-(trifluoromethyl)phenyl)-1,2-dihydrooxazolo[5,4-c]quinolin-8-yl)but-3-enenitrile (8e)* The title compound was obtained similarly to **8d**. 1-allylurea was replaced with acrylonitrile. (yellow solid, yield: 82.7%). $^1$H NMR (400 MHz, DMSO-D$_6$) δ(ppm): 9.16 (d, *J* = 3.0 Hz, 1H), 8.25 (s, 1H), 8.12 (t, *J* = 8.1 Hz, 3H), 8.05 (dd, *J* = 9.1, 1.7 Hz, 1H), 8.01 – 7.95 (m, 1H), 7.51 (d, *J* = 16.6 Hz, 1H), 7.09 (s, 1H), 6.42 (d, *J* = 16.6 Hz, 1H). $^{13}$C NMR (101 MHz, DMSO-D$_6$) δ(ppm): 153.18, 149.82, 148.24, 146.64, 137.23, 135.43, 134.83, 133.26, 133.03, 132.43, 132.08, 131.74, 128.30, 127.76, 125.87, 125.50, 122.53, 118.88, 115.22, 99.21. HR-MS (ESI) m/z: calcd. for $C_{20}H_{10}F_3N_3O_2$ [M + H]$^+$: 382.0725, found: 382.0798. Mp 235–237 °C.

*methyl(E)-3-(2-oxo-1-(3-(trifluoromethyl)phenyl)-1,2-dihydrooxazolo[5,4-c]quinolin-8-yl)acrylate (8f)* The title compound was obtained similarly to **8d**. 1-allylurea was replaced with methyl acrylate. (yellow solid, yield: 82.3%). $^1$H NMR (400 MHz, DMSO-D$_6$) δ(ppm): 9.17 (d, *J* = 11.8 Hz, 1H), 8.31 (s, 1H), 8.15 (d, *J* = 8.0 Hz, 2H), 8.11 (s, 2H), 8.01 (t, *J* = 7.9 Hz, 1H), 7.37 (d, *J* = 16.0 Hz, 1H), 7.08 (s, 1H), 6.50 (d, *J* = 16.0 Hz, 1H), 3.71 (s, 3H). $^{13}$C NMR (101 MHz, DMSO-D$_6$) δ(ppm): 166.73, 153.17, 146.48, 143.43, 137.17, 135.26, 135.06, 133.39, 133.14, 132.67, 132.22, 132.14, 132.08, 131.63, 129.21, 127.75, 127.13, 121.89, 120.20, 115.33, 52.25. HR-MS (ESI) m/z: calcd. for $C_{21}H_{13}F_3N_2O_4$ [M + H]$^+$: 415.0827, found: 415.0900. Mp 243–245 °C.

*(E)-4-(6-bromo-4-((3-(trifluoromethyl)phenyl)amino)quinolin-3-yl)but-3-en-2-one* (**9**) To a solution of compound **2** (3.95 g, 10 mmol) in DMSO, then 1-(triphenylphosphoranylidene)propan-2-one (3.18 g, 10 mmol) was added. The resulting mixture was heated to 120 °C for 4 h before cooling to room temperature. The residue was diluted with water followed by extraction with EtOAc. Purification of the residue by ISCO (hexanes/EtOAc 5:1) provided compound **9** as a yellow solid. (3.79 g, 87.3% yield). ^{1}H NMR (400 MHz, DMSO-D$_6$) δ(ppm): 9.46 (s, 1H), 9.13 (s, 1H), 8.47 (d, $J$ = 1.9 Hz, 1H), 7.94 (dt, $J$ = 8.9, 5.4 Hz, 2H), 7.45 (t, $J$ = 8.3 Hz, 1H), 7.35 (d, $J$ = 16.5 Hz, 1H), 7.23 (d, $J$ = 7.7 Hz, 1H), 7.12 (d, $J$ = 5.7 Hz, 2H), 6.89 (d, $J$ = 16.5 Hz, 1H), 1.98 (s, 3H). ^{13}C NMR (101 MHz, DMSO-D$_6$) δ(ppm): 198.15, 151.28, 148.24, 145.30, 144.10, 138.46, 134.00, 132.24, 132.07, 131.98, 130.76, 129.35, 129.24, 128.30, 126.43, 124.78, 121.43, 120.32, 118.81, 27.19. HR-MS (ESI) m/z: calcd. for $C_{20}H_{14}BrF_3N_2O$ [M + H]$^+$: 435.0242, found: 435.0313. Mp 115–119 °C.

*(E)-4-(6-(6-aminopyridin-3-yl)-4-((3-(trifluoromethyl)phenyl)amino)quinolin-3-yl) but-3 -en-2-one(**10a**)* To a solution of compound **9** (4.34 g, 10 mmol) in 1,4-dioxane at room temperature, Pd(PPh$_3$)$_4$ (1.16 g, 1 mmol), K$_2$CO$_3$ (2.76 g, 20 mmol), and (4-aminophenyl) boronic acid (1.64 g, 12 mmol) were subsequently added. After degassing, the resulting mixture was heated to 80 °C for 4 h before cooling to room temperature. The solution was extracted with EtOAc. The organic layer was washed with water and brine, dried (MgSO$_4$), filtered, and evaporated to dryness as a yellow solid (3.69 g, 82.6% yield). ^{1}H-NMR (400 MHz, DMSO-D$_6$) δ (ppm): 9.52 (s, 1H), 9.12 (s, 1H), 8.43 (d, $J$ = 1.6 Hz, 1H), 8.10 (d, $J$ = 8.7 Hz, 1H), 8.02 (dd, $J$ = 8.7, 1.8 Hz, 1H), 7.48 (d, $J$ = 4.1 Hz, 1H), 7.45 (d, $J$ = 4.4 Hz, 1H), 7.24 (d, $J$ = 7.8 Hz, 1H), 7.19 – 7.14 (m, 3H), 6.98 (d, $J$ = 1.7 Hz, 1H), 6.94 – 6.88 (m, 2H), 6.65 (dd, $J$ = 8.0, 1.4 Hz, 1H), 5.24 (s, 2H), 2.03 (s, 3H). ^{13}C NMR (101 MHz, DMSO-D$_6$) δ(ppm): 198.13, 150.31, 149.74, 148.90, 145.80, 145.10, 140.66, 139.75, 138.83, 130.73, 130.46, 130.12, 130.04, 127.79, 125.98, 123.54, 121.33, 118.50, 117.20, 115.32, 114.16, 113.82, 112.95, 27.17. HR-MS (ESI) m/z: calcd. for $C_{26}H_{20}F_3N_3O$ [M + H]$^+$: 448.1558, found: 448.1632. Mp 183–185 °C.

*(E)-4-(6-(3-aminophenyl)-4-((3-(trifluoromethyl)phenyl)amino)quinolin-3-yl)but-3-en-2-one(**10b**)* The title compound was obtained similarly to **10a**. The boronic acid was replaced with (3-aminophenyl)boronic acid. (yellow solid, yield: 84.7%). ^{1}H-NMR (400 MHz, DMSO-D$_6$) δ(ppm): 9.49 (s, 1H), 9.10 (s, 1H), 8.39 (s, 1H), 8.08 (d, $J$ = 8.7 Hz, 1H), 8.00 (dd, $J$ = 8.7, 1.5 Hz, 1H), 7.45 (dd, $J$ = 15.8, 7.0 Hz, 2H), 7.22 (d, $J$ = 7.7 Hz, 1H), 7.13 (dd, $J$ = 7.9, 4.5 Hz, 3H),

6.90 (dd, $J$ = 24.7, 8.4 Hz, 3H), 6.61 (d, $J$ = 6.7 Hz, 1H), 5.22 (s, 2H), 2.01 (s, 3H). $^{13}$C NMR (101 MHz, DMSO-D$_6$) δ(ppm): 198.13, 150.33, 149.75, 148.88, 145.79, 145.10, 140.64, 139.75, 138.80, 130.76, 130.46, 130.14, 130.04, 128.69, 127.82, 125.98, 123.54, 123.27, 121.31, 118.52, 117.21, 115.28, 114.14, 113.81, 112.92, 27.21. HR-MS (ESI) m/z: calcd. for C$_{26}$H$_{20}$F$_3$N$_3$O [M + H]$^+$: 448.1558, found: 448.1630. Mp 184–186 °C.

*(E)-4-(6-(5-methoxypyridin-3-yl)-4-((3-(trifluoromethyl)phenyl)amino)quinolin-3-yl)but-3-en-2-one (10c)* The title compound was obtained similarly to **10a**. The boronic acid was replaced with (5-methoxypyridin-3-yl)boronic acid. (green solid, yield: 88.5%). $^1$H-NMR (400 MHz, DMSO-D$_6$) δ(ppm): 9.51 (s, 1H), 9.12 (s, 1H), 8.58 (dd, $J$ = 25.3, 1.4 Hz, 2H), 8.35 (d, $J$ = 2.7 Hz, 1H), 8.20 (dd, $J$ = 8.7, 1.7 Hz, 1H), 8.12 (d, $J$ = 8.7 Hz, 1H), 7.74 – 7.65 (m, 1H), 7.53 – 7.38 (m, 2H), 7.26 (d, $J$ = 7.7 Hz, 1H), 7.18 (d, $J$ = 6.9 Hz, 2H), 6.89 (d, $J$ = 16.4 Hz, 1H), 3.92 (s, 3H), 2.01 (s, 3H). $^{13}$C NMR (101 MHz, DMSO-D$_6$) δ(ppm): 198.13, 156.14, 151.01, 149.16, 145.48, 145.31, 140.70, 138.79, 137.25, 136.10, 135.29, 130.75, 130.44, 130.06, 127.88, 123.23, 123.16, 122.46, 122.03, 119.22, 118.13, 117.66, 114.50, 114.47, 56.25, 27.17. HR-MS (ESI) m/z: calcd. for C$_{26}$H$_{20}$F$_3$N$_3$O$_2$ [M + H]$^+$: 464.1508, found: 464.1580. Mp 164–167 °C.

*(E)-4-(4'-((3-(trifluoromethyl)phenyl)amino)-[3,6'-biquinolin]-3'-yl)but-3-en-2-one (10d)* The title compound was obtained similarly to **10a**. The boronic acid was replaced with quinolin-3-ylboronic acid. (yellow solid, yield: 90.9%). $^1$H-NMR (400 MHz, DMSO-D$_6$) δ(ppm): 9.57 (s, 1H), 9.38 (d, $J$ = 2.1 Hz, 1H), 9.13 (s, 1H), 8.75 (d, $J$ = 7.3 Hz, 2H), 8.34 (d, $J$ = 8.6 Hz, 1H), 8.18 (d, $J$ = 8.7 Hz, 1H), 8.13 – 8.02 (m, 2H), 7.81 (t, $J$ = 7.7 Hz, 1H), 7.68 (t, $J$ = 7.5 Hz, 1H), 7.54 – 7.35 (m, 2H), 7.28 (d, $J$ = 7.8 Hz, 1H), 7.22 (d, $J$ = 1.9 Hz, 2H), 6.89 (d, $J$ = 16.4 Hz, 1H), 2.00 (s, 3H). $^{13}$C NMR (101 MHz, DMSO-D$_6$) δ(ppm): 198.12, 151.01, 150.08, 149.07, 147.47, 145.48, 145.40, 138.91, 135.49, 133.87, 132.53, 130.92, 130.78, 130.39, 130.14, 129.26, 128.95, 128.08, 127.85, 127.77, 125.96, 123.35, 123.25, 122.47, 122.14, 118.04, 117.71, 114.58, 27.12. HR-MS (ESI) m/z: calcd. for C$_{29}$H$_{20}$F$_3$N$_3$O [M + H]$^+$: 484.1558, found: 484.1631. Mp 173–176 °C.

*(E)-4-(6-(6-fluoropyridin-3-yl)-4-((3-(trifluoromethyl)phenyl)amino)quinolin-3-yl)but-3-en-2-one (10e)* The title compound was obtained similarly to **10a**. The boronic acid was replaced with (6-fluoropyridin-3-yl)boronic acid. (yellow solid, yield: 89.3%). $^1$H-NMR (400 MHz, DMSO-D$_6$) δ(ppm): 10.22 (s, 1H), 9.08 (s, 1H), 8.87 – 8.71 (m, 2H), 8.51 (td, $J$ = 8.3, 2.7 Hz, 1H), 8.24 (dd, $J$ = 8.8, 1.8 Hz, 1H), 8.13 (d, $J$ = 8.7 Hz, 1H), 7.54 (t, $J$ = 7.8 Hz, 1H), 7.45 – 7.26

(m, 4H), 7.20 (d, $J$ = 16.4 Hz, 1H), 6.79 (d, $J$ = 16.4 Hz, 1H), 1.92 (d, $J$ = 3.9 Hz, 3H). $^{13}$C NMR (101 MHz, DMSO-D$_6$) δ(ppm): 197.97, 162.22, 149.07, 147.65, 146.57, 146.42, 144.28, 141.27, 141.19, 138.71, 134.70, 133.55, 130.74, 128.03, 125.85, 123.76, 123.14, 122.56, 122.46, 119.10, 116.46, 116.28, 110.51, 110.14, 26.83. HR-MS (ESI) m/z: calcd. for C$_{25}$H$_{17}$F$_4$N$_3$O [M + H]$^+$: 452.1308, found: 452.1381. Mp 133–134 °C.

*9-(2-fluoropyridin-3-yl)-1-(3-(trifluoromethyl)phenyl)benzo[h][1,6]naphthyridin-2(1H)-one* *(11a)* The title compound was obtained similarly to **4a**. The boronic acid was replaced with (2-fluoropyridin-3-yl)boronic acid. (white solid, yield: 89.9%). $^1$H NMR (400 MHz, DMSO-D$_6$) δ(ppm): 9.22 (s, 1H), 8.36 (d, $J$ = 9.5 Hz, 1H), 8.29 – 8.22 (m, 1H), 8.16 (d, $J$ = 8.7 Hz, 1H), 8.09 (s, 1H), 7.99 – 7.89 (m, 2H), 7.89 – 7.77 (m, 2H), 7.53 – 7.45 (m, 1H), 7.44 – 7.35 (m, 1H), 6.98 (dd, $J$ = 9.5, 3.8 Hz, 1H), 6.89 (d, $J$ = 1.7 Hz, 1H). $^{13}$C NMR (101 MHz, DMSO-D$_6$) δ(ppm): 163.07, 160.88, 158.52, 152.23, 148.89, 147.72, 147.57, 142.59, 141.67, 141.39, 140.79, 133.83, 132.02, 131.21, 130.99, 130.65, 126.98, 126.59, 125.99, 122.94, 122.48, 122.26, 117.64, 114.15. HR-MS (ESI) m/z: calcd. for C$_{24}$H$_{13}$F$_4$N$_3$O [M + H]$^+$: 436.0995, found: 436.1068. Mp 158–161 °C.

*9-(6-fluoropyridin-3-yl)-1-(3-(trifluoromethyl)phenyl)benzo[h][1,6]naphthyridin-2(1H)-one* *(11b)* The title compound was obtained similarly to **4a**. The boronic acid was replaced with (6-fluoropyridin-3-yl)boronic acid. (white solid, yield: 87.6%). $^1$H NMR (400 MHz, DMSO-D$_6$) δ(ppm): 9.19 (s, 1H), 8.36 (d, $J$ = 9.5 Hz, 1H), 8.15 (d, $J$ = 8.7 Hz, 2H), 8.09 – 8.00 (m, 2H), 7.97 – 7.86 (m, 2H), 7.84 (d, $J$ = 8.0 Hz, 1H), 7.69 (td, $J$ = 8.2, 2.7 Hz, 1H), 7.23 (dd, $J$ = 8.5, 2.8 Hz, 1H), 6.96 (dd, $J$ = 14.4, 5.6 Hz, 2H). $^{13}$C NMR (101 MHz, DMSO-D$_6$) δ(ppm): 163.05, 151.97, 148.96, 145.77, 145.61, 142.48, 141.89, 140.80, 140.60, 140.52, 134.08, 133.70, 133.13, 132.14, 131.75, 129.11, 127.14, 126.70, 123.55, 122.47, 117.79, 114.19, 110.36, 109.99. HR-MS (ESI) m/z: calcd. for C$_{24}$H$_{13}$F$_4$N$_3$O [M + H]$^+$: 436.0995, found: 436.1068. Mp 264–266 °C.

*9-(2-methoxypyridin-3-yl)-1-(3-(trifluoromethyl)phenyl)benzo[h][1,6]naphthyridin-2(1H)-one* *(11c)* The title compound was obtained similarly to **4a**. The boronic acid was replaced with (2-methoxypyridin-3-yl)boronic acid. (white solid, yield: 88.2%). $^1$H NMR (400 MHz, DMSO-D$_6$) δ(ppm): 9.18 (s, 1H), 8.35 (d, $J$ = 9.5 Hz, 1H), 8.17 (dd, $J$ = 4.8, 2.1 Hz, 1H), 8.11 – 8.05 (m, 2H), 7.96 – 7.88 (m, 2H), 7.87 – 7.76 (m, 2H), 7.05 – 6.92 (m, 3H), 6.80 (d, $J$ = 1.7 Hz, 1H), 3.81 (s, 3H). $^{13}$C NMR (101 MHz, DMSO-D$_6$) δ(ppm): 163.10, 160.34, 151.69, 148.64, 147.02, 142.48, 141.86, 140.83, 138.76, 134.06, 133.95, 131.99, 131.42, 131.11, 130.30, 126.99,

126.49, 125.75, 123.11, 122.82, 122.24, 117.62, 117.51, 113.99, 53.90. HR-MS (ESI) m/z: calcd. for $C_{25}H_{16}F_3N_3O_2$ [M + H]$^+$: 448.1195, found: 448.1268. Mp 272–275 °C.

*9-(6-methoxypyridin-3-yl)-1-(3-(trifluoromethyl)phenyl)benzo[h][1,6]naphthyridin-2(1H)-one (11d)* The title compound was obtained similarly to **4a**. The boronic acid was replaced with (6-methoxypyridin-3-yl)boronic acid. (white solid, yield: 87.4%). $^1$H NMR (400 MHz, DMSO-D$_6$) δ(ppm): 9.16 (s, 1H), 8.34 (d, *J* = 9.5 Hz, 1H), 8.16 – 8.08 (m, 2H), 8.07 – 7.96 (m, 3H), 7.89 (t, *J* = 7.9 Hz, 1H), 7.81 (d, *J* = 8.0 Hz, 1H), 7.28 (dd, *J* = 8.7, 2.6 Hz, 1H), 6.94 (dd, *J* = 10.5, 5.6 Hz, 2H), 6.80 (dd, *J* = 8.6, 0.4 Hz, 1H), 3.88 (s, 3H). $^{13}$C NMR (101 MHz, DMSO-D$_6$) δ(ppm): 163.76, 163.08, 151.50, 148.67, 145.35, 142.37, 141.95, 140.81, 137.55, 134.32, 133.93, 132.12, 131.57, 131.28, 128.83, 128.61, 127.20, 126.68, 125.58, 122.70, 122.34, 117.88, 114.13, 110.92, 53.90. HR-MS (ESI) m/z: calcd. for $C_{25}H_{16}F_3N_3O_2$ [M + H]$^+$: 448.1195, found: 448.1267. Mp 211–216 °C.

*N-(5-(2-oxo-1-(3-(trifluoromethyl)phenyl)-1,2-dihydrobenzo[h][1,6]naphthyridin-9-yl)pyridin e-2-yl) propionamide (11e)* The title compound was obtained similarly to **4a**. The boronic acid was replaced with (6-propionamidopyridin-3-yl)boronic acid. (white solid, yield: 90.9%). $^1$H NMR (400 MHz, DMSO-D$_6$) δ(ppm): 10.64 (s, 1H), 9.18 (s, 1H), 8.35 (d, *J* = 9.5 Hz, 1H), 8.07 (ddd, *J* = 16.3, 11.5, 5.5 Hz, 6H), 7.96 – 7.83 (m, 2H), 7.49 (dd, *J* = 8.7, 2.5 Hz, 1H), 6.99 (dd, *J* = 22.2, 5.5 Hz, 2H), 2.43 (q, *J* = 7.5 Hz, 2H), 1.08 (t, *J* = 7.5 Hz, 3H). $^{13}$C NMR (101 MHz, DMSO-D$_6$) δ(ppm): 173.64, 163.08, 152.34, 151.49, 148.56, 145.94, 142.49, 141.94, 140.82, 136.41, 134.14, 132.06, 131.63, 131.52, 131.31, 130.07, 128.94, 128.78, 127.07, 126.56, 125.58, 122.44, 117.89, 114.14, 113.41, 29.80, 9.89. HR-MS (ESI) m/z: calcd. for $C_{27}H_{19}F_3N_4O_2$ [M + H]$^+$: 489.1460, found: 489.1533. Mp 249–250 °C.

*N-(5-(2-oxo-1-(3-(trifluoromethyl)phenyl)-1,2-dihydrobenzo[h][1,6]naphthyridin-9-yl)pyridin -2-yl)butyramide (11f)* The title compound was obtained similarly to **4a**. The boronic acid was replaced with (6-butyramidopyridin-3-yl)boronic acid. (white solid, yield: 81.9%). $^1$H NMR (400 MHz, DMSO-D$_6$) δ(ppm): 10.65 (s, 1H), 9.16 (s, 1H), 8.34 (d, *J* = 9.5 Hz, 1H), 8.12 (d, *J* = 8.8 Hz, 3H), 8.08 – 7.97 (m, 3H), 7.96 – 7.82 (m, 2H), 7.49 (dd, *J* = 8.7, 2.5 Hz, 1H), 6.99 (dd, *J* = 24.4, 5.5 Hz, 2H), 2.40 (t, *J* = 7.3 Hz, 2H), 1.69 – 1.55 (m, 2H), 0.92 (t, *J* = 7.4 Hz, 3H). $^{13}$C NMR (101 MHz, DMSO-D$_6$) δ(ppm): 172.82, 163.08, 152.30, 151.60, 148.78, 145.94, 142.37, 141.96, 140.82, 136.40, 134.08, 132.05, 131.68, 131.30, 130.13, 128.87, 127.05, 126.54, 125.58,

122.86, 122.41, 122.35, 117.88, 114.14, 113.46, 38.43, 18.86, 14.13. HR-MS (ESI) m/z: calcd. for $C_{28}H_{21}F_3N_4O_2$ [M + H]$^+$: 503.1617, found: 503.1689. Mp 279–280 °C.

*N-(5-(2-oxo-1-(3-(trifluoromethyl)phenyl)-1,2-dihydrobenzo[h][1,6]naphthyridin-9-yl)pyridin -2-yl)isobutyramide (**11g**)* The title compound was obtained similarly to **4a**. The boronic acid was replaced with (6-isobutyramidopyridin-3-yl)boronic acid. (white solid, yield: 82.8%). $^1$H NMR (400 MHz, DMSO-D$_6$) δ(ppm): 10.64 (s, 1H), 9.17 (s, 1H), 8.35 (d, *J* = 9.4 Hz, 1H), 8.17 – 8.09 (m, 3H), 8.09 – 8.00 (m, 3H), 7.95 – 7.84 (m, 2H), 7.48 (dd, *J* = 8.7, 2.5 Hz, 1H), 7.03 (d, *J* = 1.5 Hz, 1H), 7.00 – 6.93 (m, 1H), 2.79 (dt, *J* = 13.6, 6.8 Hz, 1H), 1.11 (d, *J* = 6.8 Hz, 6H). $^{13}$C NMR (101 MHz, DMSO-D$_6$) δ(ppm): 176.90, 163.09, 152.43, 151.62, 148.79, 145.94, 142.39, 141.97, 140.83, 136.38, 134.17, 134.07, 132.06, 131.70, 131.63, 131.30, 130.14, 128.88, 127.08, 126.56, 122.40, 120.17, 117.90, 114.14, 113.53, 34.97, 19.91. HR-MS (ESI) m/z: calcd. for $C_{28}H_{21}F_3N_4O_2$ [M + H]$^+$: 503.1617, found: 503.1689. Mp 213–215 °C.

*N-(5-(2-oxo-1-(3-(trifluoromethyl)phenyl)-1,2-dihydrobenzo[h][1,6]naphthyridin-9-yl)pyridin -2-yl)pentanamide (**11h**)* The title compound was obtained similarly to **4a**. The boronic acid was replaced with (6-pentanamidopyridin-3-yl)boronic acid. (white solid, yield: 86.3%). $^1$H NMR (400 MHz, DMSO-D$_6$) δ(ppm): 10.64 (s, 1H), 9.17 (s, 1H), 8.35 (d, *J* = 9.5 Hz, 1H), 8.12 (dd, *J* = 8.5, 6.3 Hz, 3H), 8.08 – 7.97 (m, 3H), 7.96 – 7.83 (m, 2H), 7.49 (dd, *J* = 8.7, 2.5 Hz, 1H), 7.03 (d, *J* = 1.6 Hz, 1H), 6.96 (d, *J* = 9.4 Hz, 1H), 2.42 (t, *J* = 7.4 Hz, 2H), 1.63 – 1.51 (m, 2H), 1.32 (dq, *J* = 14.6, 7.3 Hz, 2H), 0.97 – 0.85 (m, 3H). $^{13}$C NMR (101 MHz, DMSO-D$_6$) δ(ppm): 172.97, 163.08, 152.31, 151.62, 148.79, 145.95, 142.39, 141.97, 140.83, 136.41, 134.15, 134.10, 132.06, 131.70, 131.62, 131.30, 130.14, 128.90, 127.06, 126.58, 122.43, 122.36, 117.90, 114.15, 113.46, 36.25, 27.56, 22.30, 14.29. HR-MS (ESI) m/z: calcd. for $C_{29}H_{23}F_3N_4O_2$ [M + H]$^+$: 517.1773, found: 517.1846. Mp 274–277 °C.

*N-(5-(2-oxo-1-(3-(trifluoromethyl)phenyl)-1,2-dihydrobenzo[h][1,6]naphthyridin-9-yl)pyridin -2-yl)-2-phenylacetamide (**11i**)* The title compound was obtained similarly to **4a**. The boronic acid was replaced with (6-(2-phenylacetamido)pyridin-3-yl)boronic acid. (white solid, yield: 83.7%). $^1$H NMR (400 MHz, DMSO-D$_6$) δ(ppm): 10.94 (s, 1H), 9.17 (s, 1H), 8.34 (d, *J* = 9.5 Hz, 1H), 8.18 – 7.99 (m, 6H), 7.94 – 7.82 (m, 2H), 7.49 (dd, *J* = 8.7, 2.5 Hz, 1H), 7.43 – 7.29 (m, 4H), 7.30 – 7.22 (m, 1H), 7.02 (d, *J* = 1.7 Hz, 1H), 6.96 (d, *J* = 9.4 Hz, 1H), 3.76 (s, 2H). $^{13}$C NMR (101 MHz, DMSO-D$_6$) δ(ppm): 170.78, 163.08, 152.21, 151.64, 148.77, 146.02, 142.41, 141.96, 140.83, 136.50, 136.23, 134.15, 134.01, 132.07, 131.68, 131.30, 130.41, 129.77, 128.86,

127.16, 127.08, 126.55, 125.58, 122.87, 122.49, 122.37, 117.90, 114.14, 113.47, 43.44. HR-MS (ESI) m/z: calcd. for $C_{32}H_{21}F_3N_4O_2$ [M + H]$^+$: 551.1617, found: 551.1689. Mp 143–145 °C.

*Tert-butyl(5-(2-oxo-1-(3-(trifluoromethyl)phenyl)-1,2-dihydrobenzo[h][1,6]naphthyridin-9-yl) pyridin-2-yl)carbamate (11j)* The title compound was obtained similarly to **4a**. The boronic acid was replaced with (6-((tert-butoxycarbonyl)amino)pyridin-3-yl)boronic acid. (white solid, yield: 85.6%). $^1$H NMR (400 MHz, DMSO-D$_6$) δ(ppm): 10.02 (s, 1H), 9.16 (s, 1H), 8.35 (d, *J* = 9.5 Hz, 1H), 8.12 (dd, *J* = 11.2, 2.3 Hz, 3H), 8.04 (dt, *J* = 8.8, 4.4 Hz, 2H), 7.91 (t, *J* = 7.8 Hz, 1H), 7.82 (dd, *J* = 17.8, 8.4 Hz, 2H), 7.33 (dd, *J* = 8.8, 2.5 Hz, 1H), 6.98 (dd, *J* = 14.7, 5.6 Hz, 2H), 1.50 (s, 9H). $^{13}$C NMR (101 MHz, DMSO-D$_6$) δ(ppm): 163.08, 153.22, 152.68, 151.55, 148.76, 146.11, 142.37, 141.94, 140.83, 136.10, 134.19, 134.10, 132.07, 131.81, 131.65, 131.28, 129.32, 128.81, 127.09, 126.60, 122.89, 122.41, 117.91, 114.14, 112.28, 80.30, 28.54. HR-MS (ESI) m/z: calcd. for $C_{29}H_{23}F_3N_4O_3$ [M + H]$^+$: 533.1722, found: 533.1795. Mp 234–236 °C.

*Phenyl(5-(2-oxo-1-(3-(trifluoromethyl)phenyl)-1,2-dihydrobenzo[h][1,6]naphthyridin-9-yl)pyr idin-2-yl)carbamate (11k)* The title compound was obtained similarly to **4a**. The boronic acid was replaced with (6-((phenoxycarbonyl)amino)pyridin-3-yl)boronic acid. (white solid, yield: 83.3%). $^1$H NMR (400 MHz, DMSO-D$_6$) δ(ppm): 10.98 (s, 1H), 9.19 (d, *J* = 10.9 Hz, 1H), 8.35 (dt, *J* = 11.1, 5.6 Hz, 1H), 8.22 – 8.10 (m, 3H), 8.08 – 8.02 (m, 1H), 7.90 (ddd, *J* = 14.7, 13.6, 7.7 Hz, 3H), 7.47 (ddd, *J* = 11.5, 9.8, 5.8 Hz, 3H), 7.38 – 7.21 (m, 4H), 7.03 (d, *J* = 1.9 Hz, 1H), 6.97 (dd, *J* = 9.4, 1.3 Hz, 1H). $^{13}$C NMR (101 MHz, DMSO-D$_6$) δ(ppm): 163.08, 152.54, 152.07, 151.66, 150.82, 150.60, 150.53, 148.83, 147.05, 146.22, 142.41, 141.96, 140.83, 137.51, 136.51, 134.10, 132.10, 131.70, 130.30, 130.01, 128.87, 127.13, 126.24, 122.57, 121.87, 117.91, 115.72, 114.16, 112.60. HR-MS (ESI) m/z: calcd. for $C_{31}H_{19}F_3N_4O_3$ [M + H]$^+$: 553.1409, found: 553.1482. Mp 150–152 °C.

*Benzyl(5-(2-oxo-1-(3-(trifluoromethyl)phenyl)-1,2-dihydrobenzo[h][1,6]naphthyridin-9-yl)pyr idin-2-yl)carbamate (11l)* The title compound was obtained similarly to **4a**. The boronic acid was replaced with (6-(((benzyloxy)carbonyl)amino)pyridin-3-yl)boronic acid. (yellow solid, yield: 82.7%). $^1$H NMR (400 MHz, DMSO-D$_6$) δ(ppm): 10.49 (s, 1H), 9.19 (d, *J* = 14.3 Hz, 1H), 8.35 (d, *J* = 9.5 Hz, 1H), 8.27 – 7.94 (m, 5H), 7.94 – 7.73 (m, 3H), 7.61 – 7.19 (m, 6H), 7.08 – 6.88 (m, 2H), 5.21 (s, 2H). $^{13}$C NMR (101 MHz, DMSO-D$_6$) δ(ppm): 163.08, 153.99, 152.38, 151.60, 148.79, 148.72, 146.14, 142.39, 141.95, 140.82, 137.01, 136.37, 134.10, 132.08, 131.67, 131.28, 129.74, 128.99, 128.84, 128.55, 128.38, 128.00, 127.11, 126.59, 122.54, 122.36, 117.91, 114.15,

112.32, 66.44. HR-MS (ESI) m/z: calcd. for $C_{32}H_{21}F_3N_4O_3$ [M + H]$^+$: 567.1566, found: 567.1639. Mp 150–153 °C.

*9-(6-(4-methylpiperazin-1-yl)pyridin-3-yl)-1-(3-(trifluoromethyl)phenyl)benzo[h][1,6]naphthyridin-2(1H)-one (11m)* The title compound was obtained similarly to **4a**. The boronic acid was replaced with (6-(4-methylpiperazin-1-yl)pyridin-3-yl)boronic acid. (yellow solid, yield: 85.1%). $^1$H NMR (400 MHz, DMSO-D$_6$) δ(ppm): 9.12 (s, 1H), 8.33 (d, *J* = 9.5 Hz, 1H), 8.12 (s, 1H), 8.09 – 8.02 (m, 2H), 8.02 – 7.94 (m, 2H), 7.90 (t, *J* = 7.9 Hz, 1H), 7.81 (d, *J* = 8.0 Hz, 1H), 7.11 (dd, *J* = 8.9, 2.6 Hz, 1H), 6.94 (dd, *J* = 5.6, 3.8 Hz, 2H), 6.78 (d, *J* = 8.9 Hz, 1H), 3.56 – 3.46 (m, 4H), 2.45 – 2.31 (m, 4H), 2.23 (s, 3H).$^{13}$C NMR (101 MHz, DMSO-D$_6$) δ(ppm): 163.12, 158.84, 151.02, 148.40, 146.18, 142.22, 141.98, 140.83, 135.75, 134.98, 133.97, 132.04, 131.61, 131.46, 131.28, 128.41, 127.09, 126.64, 123.77, 122.22, 121.39, 117.98, 114.10, 107.06, 54.84, 46.35, 44.95. HR-MS (ESI) m/z: calcd. for $C_{29}H_{24}F_3N_5O$ [M + H]$^+$: 516.1933, found: 516.2006. Mp 161–162 °C.

*9-(6-morpholinopyridin-3-yl)-1-(3-(trifluoromethyl)phenyl)benzo[h][1,6]naphthyridin-2(1H)-one (11n)* The title compound was obtained similarly to **4a**. The boronic acid was replaced with (6-morpholinopyridin-3-yl)boronic acid. (yellow solid, yield: 84.2%). $^1$H NMR (400 MHz, DMSO-D$_6$) δ(ppm): 9.12 (s, 1H), 8.33 (d, *J* = 9.5 Hz, 1H), 8.13 (s, 1H), 8.06 (dd, *J* = 8.2, 5.0 Hz, 2H), 8.03 – 7.95 (m, 2H), 7.90 (t, *J* = 7.9 Hz, 1H), 7.81 (d, *J* = 8.0 Hz, 1H), 7.15 (dd, *J* = 8.9, 2.6 Hz, 1H), 6.94 (dd, *J* = 5.6, 3.9 Hz, 2H), 6.79 (d, *J* = 8.9 Hz, 1H), 3.81 – 3.65 (m, 4H), 3.57 – 3.42 (m, 4H). $^{13}$C NMR (101 MHz, DMSO-D$_6$) δ(ppm): 163.11, 158.98, 151.06, 148.42, 146.13, 142.23, 141.98, 140.83, 135.80, 134.89, 133.95, 132.05, 131.94, 131.46, 131.29, 128.44, 127.08, 126.61, 124.29, 122.23, 121.48, 117.97, 114.10, 107.05, 66.42, 45.45. HR-MS (ESI) m/z: calcd. for $C_{28}H_{21}F_3N_4O_2$ [M + H]$^+$: 503.1617, found: 503.1689. Mp 286–287 °C.

*9-(6-(pyrrolidin-1-yl)pyridin-3-yl)-1-(3-(trifluoromethyl)phenyl)benzo[h][1,6]naphthyridin-2(1H)-one (11o)* The title compound was obtained similarly to **4a**. The boronic acid was replaced with (6-(pyrrolidin-1-yl)pyridin-3-yl)boronic acid. (yellow solid, yield: 83.3%). $^1$H NMR (400 MHz, DMSO-D$_6$) δ(ppm): 9.10 (s, 1H), 8.32 (d, *J* = 9.5 Hz, 1H), 8.13 (s, 1H), 8.10 – 7.98 (m, 3H), 7.98 – 7.85 (m, 2H), 7.79 (d, *J* = 8.0 Hz, 1H), 7.02 (dd, *J* = 8.8, 2.6 Hz, 1H), 6.92 (dd, *J* = 10.8, 5.6 Hz, 2H), 6.36 (d, *J* = 8.8 Hz, 1H), 3.40 (t, *J* = 6.5 Hz, 4H), 1.95 (t, *J* = 6.6 Hz, 4H). $^{13}$C NMR (101 MHz, DMSO-D$_6$) δ(ppm): 163.12, 156.77, 150.79, 148.24, 146.66, 142.15, 141.98, 140.83, 135.49, 135.13, 133.86, 132.03, 131.57, 131.37, 131.24, 128.29, 127.15, 126.64, 122.16,

122.07, 120.98, 118.01, 114.08, 106.46, 46.96, 25.51. HR-MS (ESI) m/z: calcd. for $C_{28}H_{21}F_3N_4O$ [M + H]$^+$: 487.1667, found: 487.1741. Mp 252–254 °C.

## 4.2. Biological Evaluations

### 4.2.1. *In vitro* Antiviral Assay

The test compound and the positive compound were dissolved in DMSO to 100 mM depending on the mass and molecular weight of the test compound and positive compound. The test compound was diluted to a concentration of 800 μM using a cell maintenance solution and then diluted by a dilution factor of 3 times for a total of 10 concentrations. The cell maintenance medium (DMEM medium with 2% FBS) was used to serially dilute the positive drug Torin2 to the same dilution as the compound to be tested. The diluted compound was then added to a white-walled clear bottom 96-well plate at 50 μl per well. An equal volume of cell maintenance medium was added to both the cell control group and the virus control group. The EV71 virus strains were removed from -80 °C and equilibrated to room temperature. The virus was diluted to 100 TCID$_{50}$ using the maintenance medium and was then added to the above 96-well plate cells at 50 μl per well. The cell control group was added with an equal volume of maintenance medium. The RD cells were seeded at a concentration of $1 \times 10^5$ / ml in a 96-well plate with a white-walled clear bottom, 100 μl per well, and finally a volume of 200 μl per well, and the final concentration of the drug was 0.25 times that of the pretreatment concentration. The plates were cultured at 37 °C for 4 days. The buffer and substrate of the CellTiter-Glo® Chemiluminescent Cell Viability Assay reagent (Promega) were mixed in the dark to prepare a working solution, and cell viability assay were performed according to the manufacturer's protocol. The IC$_{50}$ (50% inhibitory concentration) was calculated using software Origin 8.0.

### 4.2.2. mTOR Enzyme Assay

The mTOR kinase activities of all the compounds were determined using a LanthaScreen Kinase Activity Assay (Invitrogen) following the manufacturer's instructions, with compound Torin 2 as a positive control. Briefly, the mTOR enzyme (0.5 µg/mL, Invitrogen), ATP (3 µM, Sigma), GFP-4E-BP1 peptide (0.4 µM, Invitrogen) and test compounds were diluted in kinase buffer (50 mM HEPES pH 7.5, 1 mM EGTA, 10 mM MnCl$_2$, 2 mM DTT and 0.01% Tween-20). The reactions were performed in black 384-well proxiplates (PerkinElmer) at room temperature for 1 h and stopped by adding EDTA to 10 mM. Tb-p4E-BP1 (pThr46) antibody (Invitrogen) was then added to each well to a final concentration of 2 nM, and the mixture was incubated at

room temperature for 30 min. The intensity of the light emission was measured with an Envision 2104 reader (PerkinElmer) in TR-FRET mode (excitation at 340 nm and emission at 495 nm/520 nm). All of the compounds were tested in duplicate, and the results were expressed as $IC_{50}$.

### 4.2.3. Western Blot Analysis

Cell lysates were prepared in loading buffer (Beyotime) and heated at 100 °C for 10 min, and proteins were then separated by gel electrophoresis using the NuPAGE Novex 4–12% Bis-Tris gel system. Proteins were then transferred onto a PVDF membrane using the Bio-Rad transmembrane system. The PVDF membranes were then probed with a rabbit anti-p70 S6 antibody (CST, 2708), a rabbit anti-phospho-p70 S6 antibody (CST, 9234), a rabbit anti-Akt antibody (CST, 4691), a rabbit anti- phosphor-Akt antibody (CST, 4058), or a rabbit anti-Actin antibody (CST, 4970) and visualized using the corresponding IRDye anti-rabbit antibody (LI-COR, 926-32211). The membrane was then scanned using the LI-COR Odyssey.

### 4.2.4. Molecular Modeling

The molecular docking process was as follows: first, crystal structures of mTOR were downloaded from the RCSB Protein Data Bank (http://www.rcsb.org). The selected protein Data Bank (PDB) ID was mTOR (4JSV, resolution 3.5 Å). Next, the water molecules in the crystal were cleared, and hydrogen atoms and electric charges were added. Subsequently, molecule structures of ligands were drawn by ChemBioDraw 12.0 (PerkinElmer) and introduced into protein crystal cells. Finally, the molecular docking was carried out by using the LIB-DOCK module of the Discovery Studio 2.5 package. After the docking process was finished, the best conformation (**Figure 4**) was selected and the hydrogen bonds were displayed according to the docking result.

### References

[1] S. Esposito, N. Principi, Hand, foot and mouth disease: current knowledge on clinical manifestations, epidemiology, aetiology and prevention, European Journal of Clinical Microbiology & Infectious Diseases, 37 (2018) 1-8.
[2] W.M. Koh, T. Bogich, K. Siegel, J. Jin, E.Y. Chong, C.Y. Tan, M.I. Chen, P. Horby, A.R.

Cook, The Epidemiology of Hand, Foot and Mouth Disease in Asia: A Systematic Review and Analysis, Pediatric Infectious Disease Journal, 35 (2016) e285-e300.

[3] C. Wang, H. Zhang, F. Xu, Y. Niu, Y. Wu, X. Wang, Y. Peng, J. Sun, L. Liang, P. Xu, Substituted 3-benzylcoumarins as allosteric MEK1 inhibitors: design, synthesis and biological evaluation as antiviral agents, Molecules, 18 (2013) 6057-6091.

[4] M. Gao, H. Duan, J. Liu, H. Zhang, X. Wang, M. Zhu, J. Guo, Z. Zhao, L. Meng, Y. Peng, The multi-targeted kinase inhibitor sorafenib inhibits enterovirus 71 replication by regulating IRES-dependent translation of viral proteins, Antiviral Res, 106 (2014) 80-85.

[5] W. Shi, X. Hou, H. Peng, L. Zhang, Y. Li, Z. Gu, Q. Jiang, M. Shi, Y. Ji, J. Jiang, MEK/ERK signaling pathway is required for enterovirus 71 replication in immature dendritic cells, Virology Journal,11,1(2014-12-30), 11 (2014) 227:1-13.

[6] R.L. Kuo, S.R. Shih, Strategies to develop antivirals against enterovirus 71, Virology Journal, 10 (2013) 1-8.

[7] G. Lu, J. Qi, Z. Chen, X. Xu, F. Gao, D. Lin, W. Qian, H. Liu, H. Jiang, J. Yan, G.F. Gao, Enterovirus 71 and coxsackievirus A16 3C proteases: binding to rupintrivir and their substrates and anti-hand, foot, and mouth disease virus drug design, Journal of Virology, 85 (2011) 10319-10331.

[8] T.C. Chen, H.Y. Chang, P.F. Lin, J.H. Chern, T. Hsu, C.Y. Chang, S. Shih, Novel antiviral agent DTriP-22 targets RNA-dependent RNA polymerase of enterovirus 71, Antimicrobial Agents & Chemotherapy, 53 (2009) 2740-2747.

[9] H. Kang, C. Kim, D.E. Kim, J.H. Song, M. Choi, K. Choi, M. Kang, K. Lee, H.S. Kim, J.S. Shin, Synergistic antiviral activity of gemcitabine and ribavirin against enteroviruses, Antiviral Research, 124 (2015) 1-10.

[10] C.L. Deng, H. Yeo, H.Q. Ye, S.Q. Liu, B.D. Shang, P. Gong, S. Alonso, P.Y. Shi, B. Zhang, Inhibition of enterovirus 71 by adenosine analog NITD008, Journal of Virology, 88 (2016) 11915-11923.

[11] L. Shang, Y. Wang, J. Qing, B. Shu, L. Cao, Z. Lou, P. Gong, Y. Sun, Z. Yin, An adenosine nucleoside analogue NITD008 inhibits EV71 proliferation, Antiviral Research, 112 (2014) 47-58.

[12] H. Yang, D.G. Rudge, J.D. Koos, B. Vaidialingam, H.J. Yang, N.P. Pavletich, mTOR kinase structure, mechanism and regulation, Nature, 497 (2013) 217-223.

[13] J.Jr. Polivka, F. Janku, Molecular targets for cancer therapy in the PI3K/AKT/mTOR pathway, Pharmacology & Therapeutics, 142 (2014) 164-175.

[14] R.A. Saxton, D.M. Sabatini, mTOR Signaling in Growth, Metabolism, and Disease, Cell, 168 (2017) 960-976.

[15] L.J. Bowman, A.J. Brueckner, C.T. Doligalski, The Role of mTOR Inhibitors in the Management of Viral Infections: A Review of Current Literature, Transplantation, 102 (2018) S50-S59.

[16] Y. Shi, X. He, G. Zhu, H. Tu, Z. Liu, W. Li, S. Han, J. Yin, B. Peng, W. Liu, Coxsackievirus A16 elicits incomplete autophagy involving the mTOR and ERK pathways, Plos One, 10 (2015) e0122109:1-23.

[17] P. Rai, A. Plagov, D. Kumar, S. Pathak, K.R. Ayasolla, A.K. Chawla, P.W. Mathieson, M.A. Saleem, M. Husain, A. Malhotra, P.C. Singhal, Rapamycin-induced modulation of HIV gene transcription attenuates;progression of HIVAN, Experimental & Molecular Pathology, 94 (2013) 255-261.

[18] A. Heredia, N. Le, R.B. Gartenhaus, E. Sausville, S. Medina-Moreno, J.C. Zapata, C. Davis,

R.C. Gallo, R.R. Redfield, Targeting of mTOR catalytic site inhibits multiple steps of the HIV-1 lifecycle and suppresses HIV-1 viremia in humanized mice, Proceedings of the National Academy of Sciences of the United States of America, 112 (2015) 9412-9417.

[19] K.C. Hopkins, M.A. Tartell, C. Herrmann, B.A. Hackett, F. Taschuk, D. Panda, S.V. Menghani, L.R. Sabin, S. Cherry, Virus-induced translational arrest through 4EBP1/2-dependent decay of 5'-TOP mRNAs restricts viral infection, Proc Natl Acad Sci USA, 112 (2015) E2920-E2929.

[20] S. Pujhari, M. Kryworuchko, A.N. Zakhartchouk, Role of phosphatidylinositol-3-kinase (PI3K) and the mammalian target of rapamycin (mTOR) signalling pathways in porcine reproductive and respiratory syndrome virus (PRRSV) replication, Virus Research, 194 (2014) 138-144.

[21] B. Thaa, R. Biasiotto, K. Eng, M. Neuvonen, B. Götte, L. Rheinemann, M. Mutso, A. Utt, F. Varghese, G. Balistreri, A. Merits, T. Ahola, G.M. McInerneya, Differential Phosphatidylinositol-3-Kinase-Akt-mTOR Activation by Semliki Forest and Chikungunya Viruses Is Dependent on nsP3 and Connected to Replication Complex Internalization, Journal of Virology, 89 (2016) 11420-11437.

[22] D.F. Pinelli, B.S. Wakeman, M.E. Wagener, S.H. Speck, M.L. Ford, Rapamycin Ameliorates the CTLA4-Ig-Mediated Defect in CD8(+) T Cell Immunity During Gammaherpesvirus Infection, American Journal of Transplantation Official Journal of the American Society of Transplantation & the American Society of Transplant Surgeons, 15 (2015) 2576-2587.

[23] G. Liu, M. Zhong, C. Guo, M. Komatsu, J. Xu, Y. Wang, K. Kitazato, Autophagy is involved in regulating influenza A virus RNA and protein synthesis associated with both modulation of Hsp90 induction and mTOR/p70S6K signaling pathway, International Journal of Biochemistry & Cell Biology, 72 (2016) 100-108.

[24] M.A. Su, Y.T. Huang, I.T. Chen, D.Y. Lee, Y.C. Hsieh, C.Y. Li, T.H. Ng, S.Y. Liang, S.Y. Lin, S.W. Huang, Y.A. Chiang, H.T. Yu, K.H. Khoo, G.D. Chang, C.F. Lo, H.C. Wang, An invertebrate Warburg effect: a shrimp virus achieves successful replication by altering the host metabolome via the PI3K-Akt-mTOR pathway, Plos Pathogens, 10 (2014) e1004196:1-15.

[25] A.L. Adamson, B.T. Le, B.D. Siedenburg, Inhibition of mTORC1 inhibits lytic replication of Epstein-Barr virus in a cell-type specific manner, Virology Journal, 11 (2014) 110:1-10.

[26] M.C. Brown, M.I. Dobrikov, M. Gromeier, Mitogen-activated protein kinase-interacting kinase regulates mTOR/AKT signaling and controls the serine/arginine-rich protein kinase-responsive type 1 internal ribosome entry site-mediated translation and viral oncolysis, Journal of Virology, 88 (2014) 13149-13160.

[27] K.D. Shives, E.L. Beatman, M. Chamanian, C. O'Brien, J. Hobson-Peters, J.D. Beckham, West nile virus-induced activation of mammalian target of rapamycin complex 1 supports viral growth and viral protein expression, Journal of Virology, 88 (2014) 9458-9471.

[28] Q. Liang, Z. Luo, J. Zeng, W. Chen, S.S. Foo, S.A. Lee, J. Ge, S. Wang, S.A. Goldman, B.V. Zlokovic, Zika Virus NS4A and NS4B Proteins Deregulate Akt-mTOR Signaling in Human Fetal Neural Stem Cells to Inhibit Neurogenesis and Induce Autophagy, Cell Stem Cell, 19 (2016) 663-671.

[29] X.D. Pan, D.H. Gu, J.H. Mao, H. Zhu, X. Chen, B. Zheng, Y. Shan, Concurrent inhibition of mTORC1 and mTORC2 by WYE-687 inhibits renal cell carcinoma cell growth in vitro and in vivo, Plos One, 12 (2017) e0172555:1-13.

[30] H. Weber, P. Leal, S. Stein, H. Kunkel, P. García, C. Bizama, J.A. Espinoza, I. Riquelme, B. Nervi, J.C. Araya, Rapamycin and WYE-354 suppress human gallbladder cancer xenografts in

mice, Oncotarget, 6 (2015) 31877-31888.

[31] M. Rehan, An Anti-Cancer Drug Candidate OSI-027 and its Analog as Inhibitors of mTOR: Computational Insights Into the Inhibitory Mechanisms, Journal of Cellular Biochemistry, 118 (2017) 4558-4567.

[32] L. Wu, J. Zhang, H. Wu, E. Han, DNA-PKcs interference sensitizes colorectal cancer cells to a mTOR kinase inhibitor WAY-600, Biochem Biophys Res Commun, 466 (2015) 547-553.

[33] R. Mohd, A structural insight into the inhibitory mechanism of an orally active PI3K/mTOR dual inhibitor, PKI-179 using computational approaches, Journal of Molecular Graphics & Modelling, 62 (2015) 226-234.

[34] T. Liu, Q. Sun, Q. Li, H. Yang, Y. Zhang, R. Wang, X. Lin, D. Xiao, Y. Yuan, L. Chen, W. Wang, Dual PI3K/mTOR inhibitors, GSK2126458 and PKI-587, suppress tumor progression and increase radiosensitivity in nasopharyngeal carcinoma, Mol Cancer Ther, 14 (2015) 429-439.

[35] Y. Zhou, Y. Peng, H. Tang, X. He, Z. Wang, D. Hu, X. Zhou, Autophagy induction contributes to GDC-0349 resistance in head and neck squamous cell carcinoma (HNSCC) cells, Biochemical & Biophysical Research Communications, 477 (2016) 174-180.

[36] K.K. Liu, S. Bailey, D.M. Dinh, H. Lam, C. Li, P.A. Wells, M.J. Yin, A. Zou, Conformationally-restricted cyclic sulfones as potent and selective mTOR kinase inhibitors, Bioorganic & medicinal chemistry letters, 22 (2012) 5114-5117.

[37] JWT. Yates, S.V. Holt, A. Logie, K. Payne, K. Woods, R.W. Wilkinson, B.R. Davies, S.M. Guichard, A Pharmacokinetic-Pharmacodynamic model predicting tumour growth inhibition after intermittent administration with the mTOR kinase inhibitor AZD8055, British Journal of Pharmacology, 174 (2017) 2652-2661.

[38] J.E. Grilley-Olson, P.L. Bedard, A. Fasolo, M. Cornfeld, L. Cartee, A.R. Razak, L.A. Stayner, Y. Wu, R. Greenwood, R. Singh, A phase Ib dose-escalation study of the MEK inhibitor trametinib in combination with the PI3K/mTOR inhibitor GSK2126458 in patients with advanced solid tumors, Investigational New Drugs, 34 (2016) 740-749.

[39] C. Simioni, A. Cani, A.M. Martelli, G. Zauli, A.A. Alameen, S. Ultimo, G. Tabellini, J.A. McCubrey, S. Capitani, L.M. Neri, The novel dual PI3K/mTOR inhibitor NVP-BGT226 displays cytotoxic activity in both normoxic and hypoxic hepatocarcinoma cells, Oncotarget, 6 (2015) 17147-17160.

[40] R. Calero, E. Morchon, I. Martinez-Argudo, R. Serrano, Synergistic anti-tumor effect of 17AAG with the PI3K/mTOR inhibitor NVP-BEZ235 on human melanoma, Cancer Lett, 406 (2017) 1-11.

[41] B. Toosi, F. Zaker, F. Alikarami, A. Kazemi, M.T. Ardestanii, VS-5584 as a PI3K/mTOR inhibitor enhances apoptotic effects of subtoxic dose arsenic trioxide via inhibition of NF-κB activity in B cell precursor-acute lymphoblastic leukemia, Biomedicine & Pharmacotherapy, 102 (2018) 428-437.

[42] Q. Liu, J. Wang, S.A. Kang, C.C. Thoreen, W. Hur, T. Ahmed, D.M. Sabatini, N.S. Gray, Discovery of 9-(6-aminopyridin-3-yl)-1-(3-(trifluoromethyl)phenyl)benzo[h][1,6]naphthyridin-2(1H)-one (Torin2) as a potent, selective, and orally available mammalian target of rapamycin (mTOR) inhibitor for treatment of cancer, Journal of Medicinal Chemistry, 54 (2011) 1473-1480.

[43] Q. Liu, C. Xu, S. Kirubakaran, X. Zhang, W. Hur, Y. Liu, N.P. Kwiatkowski, J. Wang, K.D. Westover, P. Gao, Characterization of Torin2, an ATP-competitive inhibitor of mTOR, ATM, and ATR, Cancer Research, 73 (2013) 2574-2586.

[44] J. Tamburini, N. Chapuis, V. Bardet, S. Park, P. Sujobert, L. Willems, N. Ifrah, F. Dreyfus, P.

Mayeux, C. Lacombe, D. Bouscary, Mammalian target of rapamycin (mTOR) inhibition activates phosphatidylinositol 3-kinase/Akt by up-regulating insulin-like growth factor-1 receptor signaling in acute myeloid leukemia: rationale for therapeutic inhibition of both pathways, Blood, 111 (2008) 379-382.

[45] N. Gray, J.W. Chang, J. Zhang, C.C. Thoreen, S.W.A. Kang, D.M. Sabatini, Q. Liu, Preparation of substituted benzonaphthyridinones as mTOR modulators, 2010, WO 2010044885 A2.

[46] J.S. Albert, S. Johnstone, P. Jones, Preparation of oxazolo [5,4-c]quinolin-2-one compounds as bromodomain inhibitors, 2014, WO 2014152029 A2.

[47] P.Y. Bounaud, C.R. Smith, E.A. Jefferson, J. Hendle, P.S. Lee, A.M. Thayer, G.C. Hirst, Preparation of heterocyclic compounds as kinase modulators, 2008, WO 2008144767 A1.

[48] B.C. Askew, P.J. Coleman, M.E. Duggan, W. Halczenko, G.D. Hartman, C. Hunt, J.H. Hutchinson, R.S. Meissner, M.A. Patane, G.R. Smith, Heterocyclic-substituted carboxylic acid integrin receptor antagonists, 1999, WO 9931061 A1

[49] S. Ranjbar, N. Edraki, M. Khoshneviszadeh, A. Foroumadi, R. Miri, M. Khoshneviszadeh, Design, synthesis, cytotoxicity evaluation and docking studies of 1,2,4-triazine derivatives bearing different arylidene-hydrazinyl moieties as potential mTOR inhibitors, Research in Pharmaceutical Sciences, 13 (2018) 1-11.

[50] F. Lei, C. Sun, S. Xu, Q. Wang, Y. Ouyang, C. Chen, H. Xia, L. Wang, P. Zheng, W. Zhu, Design, synthesis, biological evaluation and docking studies of novel 2-substituted-4-morpholino-7,8-dihydro-5H-thiopyrano[4,3-d]pyrimidine derivatives as dual PI3Kα/mTOR inhibitors, European Journal of Medicinal Chemistry, 116 (2016) S0223523416302070:27-35.

[51] W. Zhu, C. Chen, C. Sun, S. Xu, C. Wu, F. Lei, H. Xia, Q. Tu, P. Zheng, Design, synthesis and docking studies of novel thienopyrimidine derivatives bearing chromone moiety as mTOR/PI3Kα inhibitors, European Journal of Medicinal Chemistry, 93 (2015) 64-73.

[52] D.D. Li, X.F. Meng, Q. Wang, P. Yu, L.G. Zhao, Z.P. Zhang, Z.Z. Wang, W. Xiao, Consensus scoring model for the molecular docking study of mTOR kinase inhibitor, Journal of Molecular Graphics & Modelling, 79 (2017) 81-87.

[53] A. Awasthi, P. Kumar, C.V. Srikanth, S. Sahi, R. Puria, Invitro Evaluation of Torin2 and 2, 6-Dihydroxyacetophenone in Colorectal Cancer Therapy, Pathology Oncology Research Por, (2017) 301-309.

[54] U. Chaube, H. Bhatt, 3D-QSAR, molecular dynamics simulations, and molecular docking studies on pyridoaminotropanes and tetrahydroquinazoline as mTOR inhibitors, Molecular Diversity, 21 (2017) 741-759.

[55] A.A.K. Al-Ashmawy, F.A. Ragab, K.M. Elokely, M.M. Anwar, O. Perez-Leal, M.C. Rico, J. Gordon, E. Bichenkov, G. Mateo, E.M.M. Kassem, Design, synthesis and SAR of new-di-substituted pyridopyrimidines as ATP-competitive dual PI3Kα/mTOR inhibitors, Bioorganic & medicinal chemistry letters, 27 (2017) 3117-3122.

[56] T. Takeda, Y. Wang, S.H. Bryant, Structural insights of a PI3K/mTOR dual inhibitor with the morpholino-triazine scaffold, Journal of Computer-Aided Molecular Design, 30 (2016) 323-330.

[57] H. Pópulo, J.M. Lopes, P. Soares, The mTOR signalling pathway in human cancer, International Journal of Molecular Sciences, 13 (2012) 1886-1918.

[58] U. Saran, M. Foti, J.F. Dufour. Cellular and molecular effects of the mTOR inhibitor everolimus, Clinical Science, 129 (2015) 895-914.

[59] M.A. Weinberg, RES-529: a PI3K/AKT/mTOR pathway inhibitor that dissociates the mTORC1 and mTORC2 complexes, Anticancer Drugs, 27 (2016) 475-487.

[60] R. Mannhold, G.I. Poda, C. Ostermann, I.V. Tetko, Calculation of Molecular Lipophilicity: State-of-the-Art and Comparison of Log P Methods on more than 96,000 Compounds, Journal of Pharmaceutical Sciences, 98 (2010) 861-893.

**Figure 1.** Design strategy of Torin2 derivatives.

**Scheme 1.** Synthesis of **4a**-**4d**[a]. **a** Reagents and conditions: (a) ethyl 2-(diethoxyphosphoryl) acetate, $K_2CO_3$, EtOH, 100 °C; (b) **4a**-**4b**: boronic ester, $K_2CO_3$, Pd(PPh$_3$)$_4$, 1,4-dioxane, 100°C; **4c**-**4d**: Pd(dba)$_3$, CsCO$_3$, 4,5-Bis(diphenylphosphino)-9,9-dimethylxanthene, 1,4-dioxane, 100°C

**Scheme 2.** Synthesis of **8a**-**8f**[a]. [a]Reagents and conditions: (c) MCPBA, $K_2CO_3$, DCM, rt; (d) NaOH (1N), 60 °C; (e) di(1H-imidazol-1-yl)methanone, THF, rt; (f) **8a**-**8c**: boronic ester, $K_2CO_3$, Pd(PPh$_3$)$_4$, 1,4-dioxane, 100 °C; **8d**-**8f**: Pd(OAc)$_2$, enamide, Tri(o-tolyl)phosphine, Et$_3$N, DMF, 100 °C.

**Scheme 3.** Synthesis of **10a**-**10e**[a]. [a]Reagents and conditions: (g) 1-(triphenyl-l5-phosphany -lidene), DMSO, 120 °C; (h) boronic ester, $K_2CO_3$, Pd(PPh$_3$)$_4$, 1,4-dioxane, 100 °C.

**Scheme 4.** Synthesis of **11a**-**11o**[a]. [a]Reagents and conditions: (i) boronic ester, $K_2CO_3$, Pd(PPh$_3$)$_4$, 1,4-dioxane, 100 °C.

**Table 1.** Anti-EV71 activities of **4a**-**4d**, **8a**-**8f**, and **10a**-**10e**

**Table 2.** Anti-EV71 activities of **11a**-**11o**

**Figure 2.** Summarized SARs of the synthesized compounds.

**Figure 3.** *In vitro* mTOR kinase inhibitory activity.

**Figure 4.** Molecular docking results of the superimposed conformation for the optimized compounds (A) Torin2 (shown in purple) and **11e** (shown in blue); (B) **11e** and **8a** (shown in yellow); (C) **11e** and **10a** (shown in green); (D) **11e** and **11d** (shown in pink); (E) **11e** and **11h** (shown in orange); (F) **11e** and **11m** (shown in brown) with the mTOR kinase complex (PDB ID code: 4JSV).

**Figure 5.** Western blot test results for the compounds

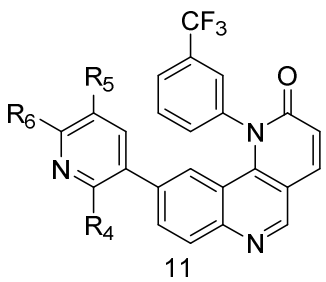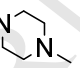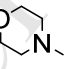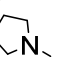**Table 3.** Absorption properties of **11a**, **11b**, **11d**, **11e** and **11m**
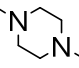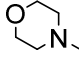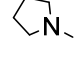
**Table 4.** Water solubility of **11a**, **11b**, **11d**, **11e** and **11m**

**Table 1.** Anti-EV71 activities of **4a**-**4d**, **8a**-**8f**, and **10a**-**10e**



| Compd. | R$_1$ | R$_2$ | R$_3$ | IC$_{50}$(μM)[a] | CC$_{50}$(μM)[b] |
|--------|-------|-------|-------|-------------------|-------------------|
| **4a** | (indolinone) | - | - | 7.40±0.18 | 10.27±7.81 |
| **4b** | (dimethylaminopyridine) | - | - | 0.27±0.05 | 0.17±0.06 |
| **4c** | (aminophenyl-HN) | - | - | 0.89±0.07 | 7.58±0.23 |
| **4d** | (aminopyridinyl-HN) | - | - | 2.47±0.11 | 5.19±0.08 |
| **8a** | - | (dimethylpyridine) | - | 4.78±0.14 | 16.88±5.46 |
| **8b** | - | (methoxypyridine) | - | >200 | 68.52±0.42 |
| **8c** | - | (quinoline) | - | >200 | 68.88±0.13 |
| **8d** | - | (urea) | - | 48.90±1.26 | 66.64±1.17 |
| **8e** | - | (NC) | - | >200 | >200 |
| **8f** | - | (ester) | - | >200 | 71.99±0.78 |
| **10a** | - | - | (H$_2$N-phenyl) | 5.14±0.54 | 5.14±1.92 |
| **10b** | - | - | (NH$_2$-phenyl) | >200 | >200 |
| **10c** | - | - | (methoxypyridine) | >200 | >200 |
| **10d** | - | - | (quinoline) | >200 | 0.68±0.21 |
| **10e** | - | - | (F-pyridine) | >200 | 2.23±0.08 |
| **Torin2** | - | - | - | 0.01±0 | 0.04±0 |

[a] The compound concentration required to reduce the virus-induced cell death by 50% was defined as $IC_{50}$. [b] The compound concentration required to reduce the cell viability to 50% of the tested control culture was defined as $CC_{50}$.

**Table 2.** Anti-EV71 activities of **11a-11o**



11a:$R_4$=F;$R_5$=$R_6$=H
11b:$R_6$=F;$R_4$=$R_5$=H
11c:$R_4$=$OCH_3$;$R_5$=$R_6$=H
11d:$R_6$=$OCH_3$;$R_4$=$R_5$=H
11e:$R_6$=$CH_3CH_2(CO)NH$;$R_4$=$R_5$=H
11f:$R_6$=$CH_3(CH_2)_2(CO)NH$;$R_4$=$R_5$=H
11g:$R_6$=$(CH_3)_2CH(CO)NH$;$R_4$=$R_5$=H
11h:$R_6$=$CH_3(CH_2)_3(CO)NH$;$R_4$=$R_5$=H
11i:$R_6$=$C_6H_5CH_2(CO)NH$;$R_4$=$R_5$=H

11j:$R_6$=$(CH_3)_3CO(CO)NH$;$R_4$=$R_5$=H
11k:$R_6$=$C_6H_5OOCNH$;$R_4$=$R_5$=H
11l:$R_6$=$C_6H_5CH_2OOCNH$;$R_4$=$R_5$=H
11m:$R_6$= [structure]  $R_4$=$R_5$=H
11n:$R_6$= [structure]  $R_4$=$R_5$=H
11o:$R_6$= [structure]  $R_4$=$R_5$=H

| Compd. | $R_4$ | $R_5$ | $R_6$ | $IC_{50}(\mu M)$ [a] | $CC_{50}(\mu M)$ [b] |
|--------|-------|-------|-------|------------------|------------------|
| **11a** | F | H | H | 0.059±0 | 1.23±1.20 |
| **11b** | H | H | F | 0.07±0.01 | 0.23±0.33 |
| **11c** | $OCH_3$ | H | H | >200 | >200 |
| **11d** | H | H | $OCH_3$ | 0.04±0.01 | 0.13±0.03 |
| **11e** | H | H | $CH_3CH_2(CO)NH$ | 0.027±0.02 | 0.04±0.02 |
| **11f** | H | H | $CH_3(CH_2)_2(CO)NH$ | 0.17±0.01 | 0.75±0.36 |
| **11g** | H | H | $(CH_3)_2CH(CO)NH$ | 0.82±0.12 | 0.46±0.03 |
| **11h** | H | H | $CH_3(CH_2)_3(CO)NH$ | 0.20±0.02 | 0.70±0.48 |
| **11i** | H | H | $C_6H_5CH_2(CO)NH$ | 0.56±0.08 | 0.74±0.72 |
| **11j** | H | H | $(CH_3)_3CO(CO)NH$ | 2.47±0.13 | 0.69±0.50 |
| **11k** | H | H | $C_6H_5OOCNH$ | 0.09±0.01 | 0.20±0.09 |
| **11l** | H | H | $C_6H_5CH_2OOCNH$ | 23.72±1.02 | 1.00±0.81 |
| **11m** | H | H | [structure] | 0.09±0.02 | 0.18±0.15 |
| **11n** | H | H | [structure] | 2.63±0.14 | 2.91±1.16 |
| **11o** | H | H | [structure] | 2.47±0.09 | 1.79±0.67 |
| **Torin2** | - | - | - | 0.01±0 | 0.04±0 |

[a] The compound concentration required to reduce the virus-induced cell death by 50% was defined as $IC_{50}$. [b] The compound concentration required to reduce the cell viability to 50% of the tested control culture was defined as $CC_{50}$.

**Table 3.** Absorption properties of **11a**, **11b**, **11d**, **11e** and **11m**

| Compd. | Property of Absorption | | | | |
|---|---|---|---|---|---|
| | MlogP[a] | S+logP[b] | S+Peff[c] | S+MDCK[d] | Absn_Risk[e] |
| **11a** | 4.024 | 4.346 | 7.883 | 1344.773 | 2.012 |
| **11b** | 4.024 | 4.422 | 8.009 | 1302.577 | 2.088 |
| **11d** | 3.744 | 4.381 | 6.418 | 1252.891 | 2.214 |
| **11e** | 3.707 | 4.001 | 4.058 | 977.619 | 1.334 |
| **11m** | 3.754 | 4.473 | 3.366 | 1282.295 | 1.683 |
| **Torin2** | 3.541 | 3.499 | 3.433 | 892.816 | 1.167 |

[a]Oil-water partition coefficient, suggested values: $-1.0 \leq MlogP \leq 4.15$. [b]Oil-water partition coefficient, suggested values: $-1.0 \leq S+logP \leq 5.0$. [c]Effective permeability in the human jejunum, suggested values: $S+Peff \geq -1.0$. [d]Apparent permeability coefficient in the Madin-Darby canine kidney cell model, suggested values: $S+MDCK \geq 30$. [e]Druggability risk about absorption, suggested values: $Absn\ Risk \leq 3$.

**Table 4.** Water solubility of **11a**, **11b**, **11d**, **11e** and **11m**

| Compd. | **Torin2** | **11a** | **11b** | **11d** | **11e** | **11m** |
|---|---|---|---|---|---|---|
| Water solubility (μg/ml) | 1.29 | 5.88 | 0.42 | 0.61 | 0.39 | 18.64 |
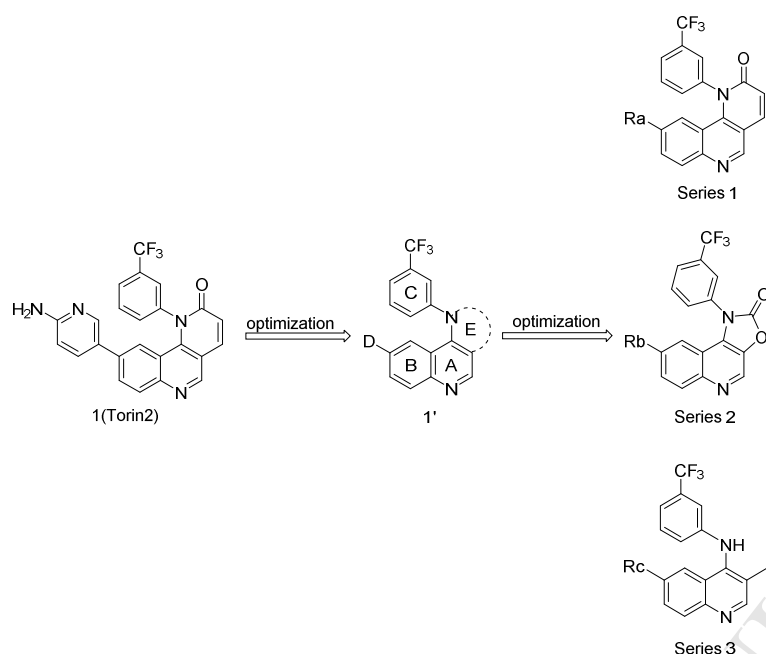
**Figure 1.** Design strategy of Torin2 derivatives.
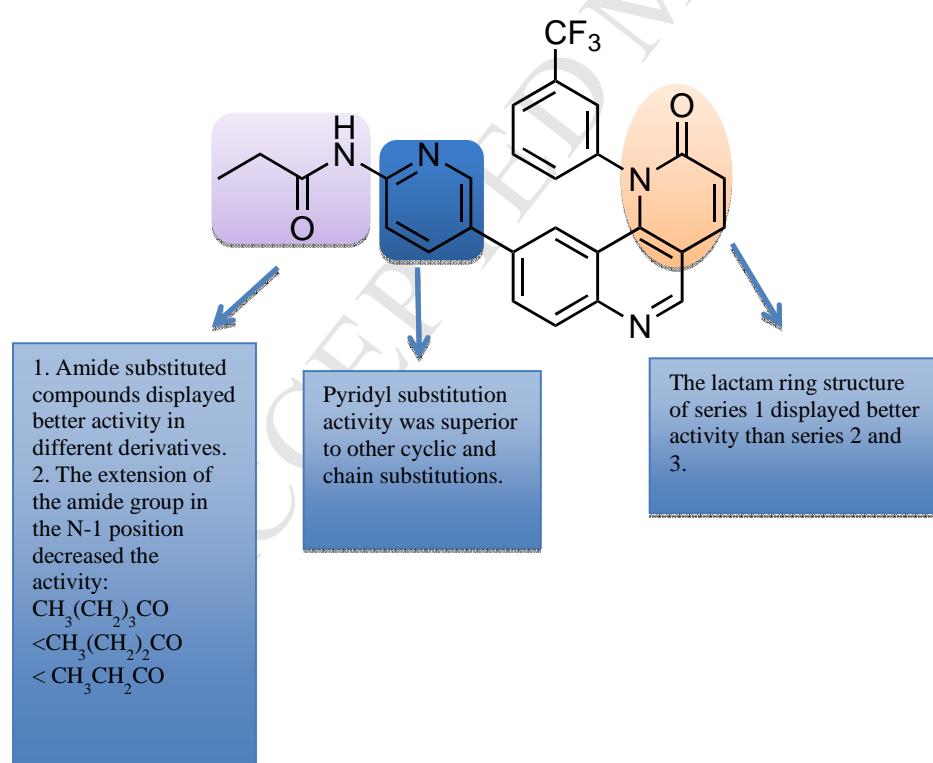


1. Amide substituted compounds displayed better activity in different derivatives.
2. The extension of the amide group in the N-1 position decreased the activity:
$CH_3(CH_2)_3CO$ $<CH_3(CH_2)_2CO$ $< CH_3CH_2CO$

Pyridyl substitution activity was superior to other cyclic and chain substitutions.

The lactam ring structure of series 1 displayed better activity than series 2 and 3.

**Figure 2.** Summarized SARs of the synthesized compounds.

**Figure 3.** *In vitro* mTOR kinase inhibitory activity.
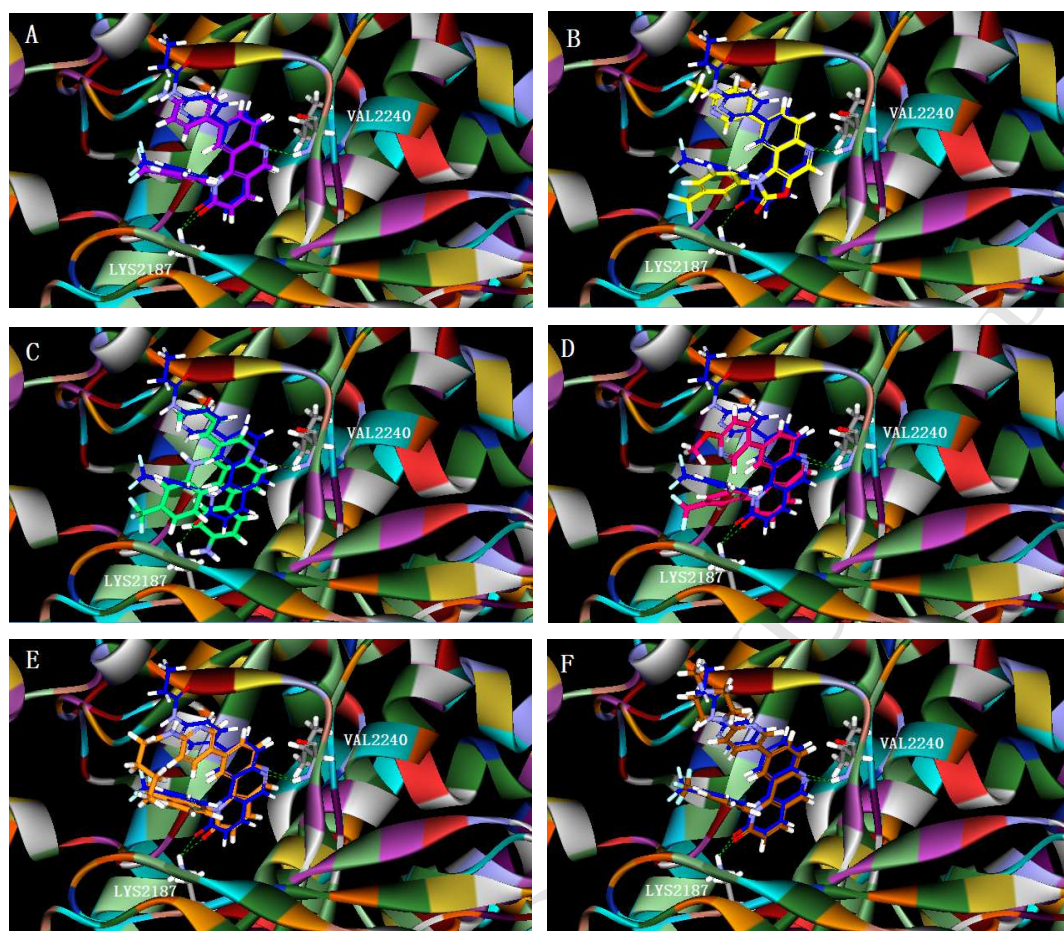
**Figure 4.** Molecular docking results of the superimposed conformation for the optimized compounds (A) Torin2 (shown in purple) and **11e** (shown in blue); (B) **11e** and **8a** (shown in yellow); (C) **11e** and **10a** (shown in green); (D) **11e** and **11d** (shown in pink); (E) **11e** and **11h** (shown in orange); (F) **11e** and **11m** (shown in brown) with the mTOR kinase complex (PDB ID code: 4JSV).
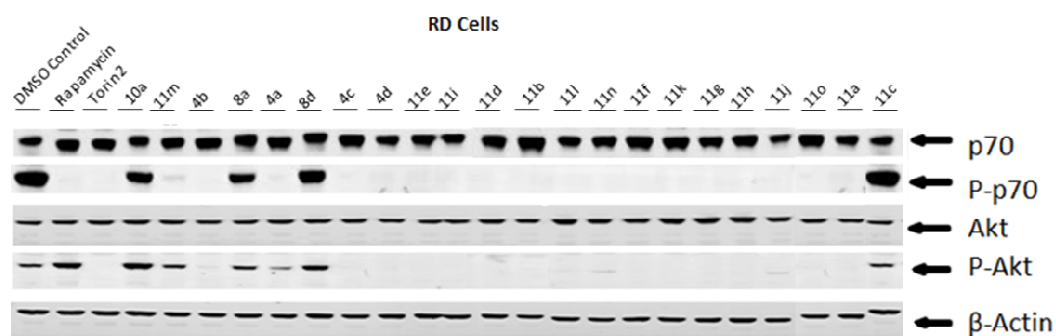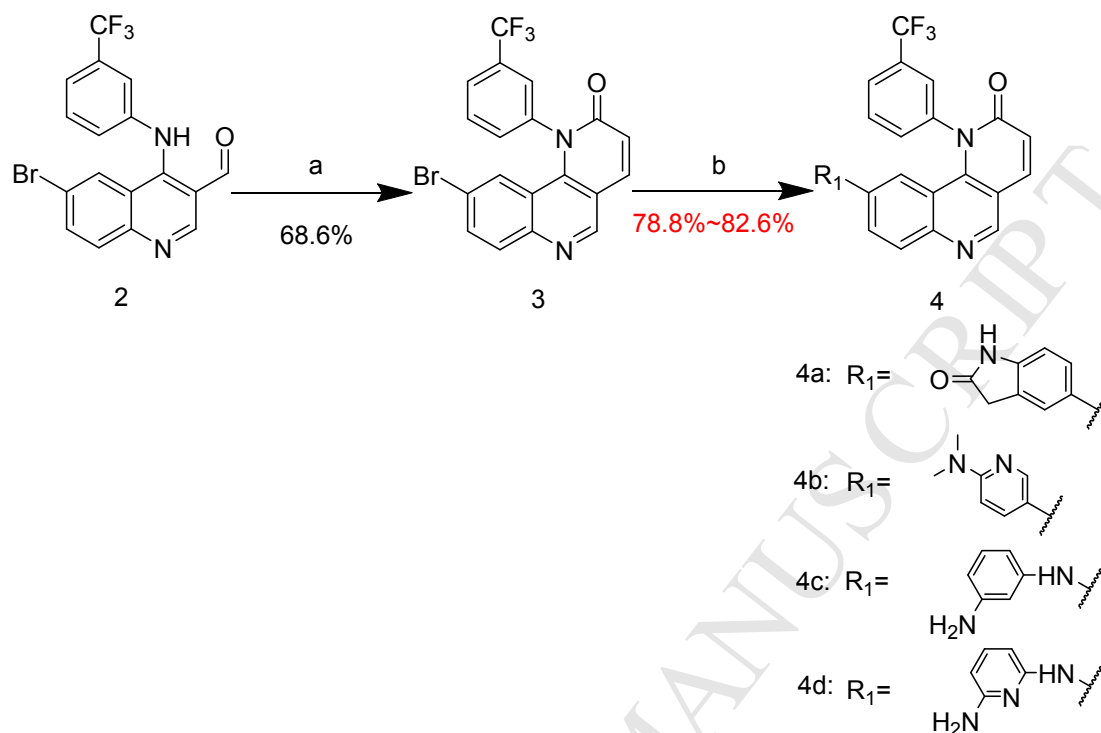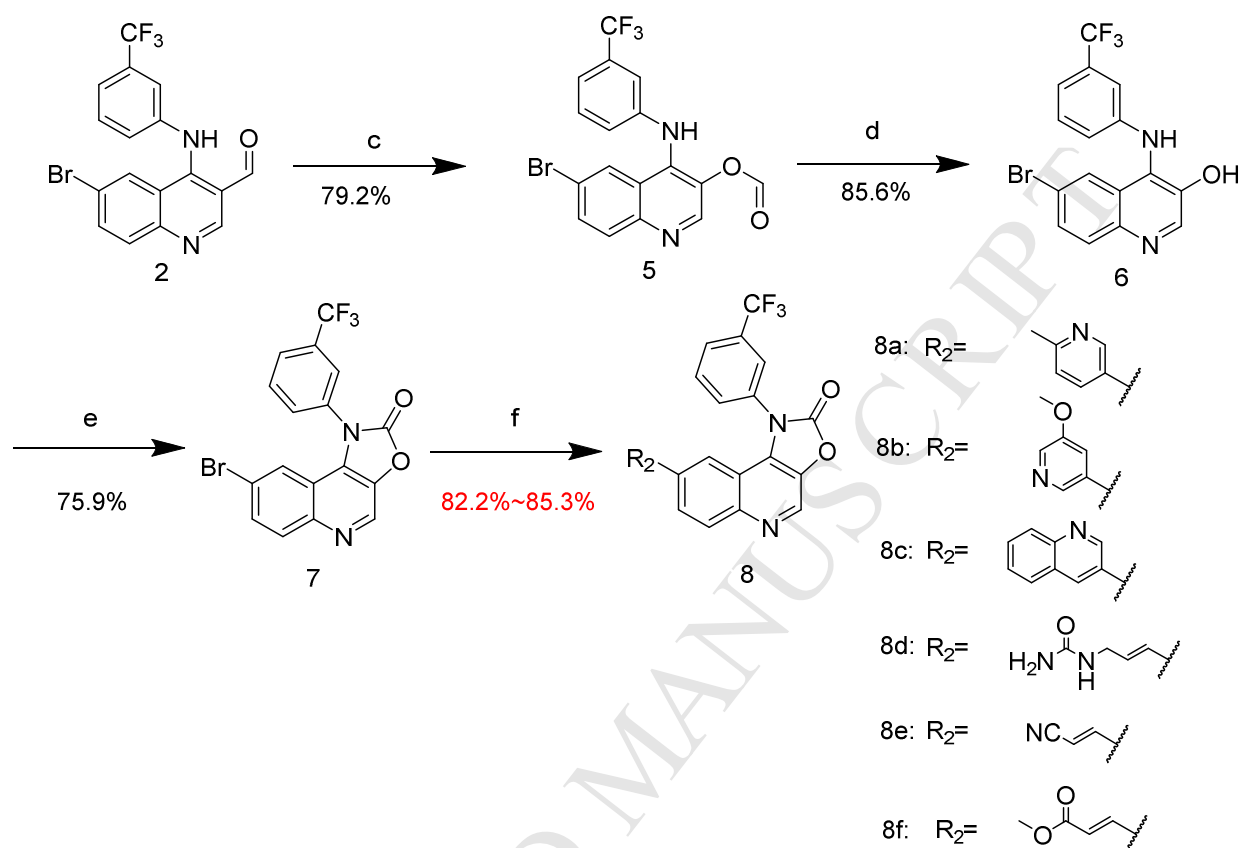


**Figure 5.** Western blot test results for the compounds
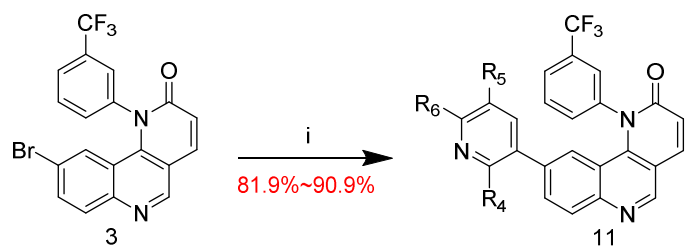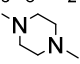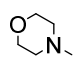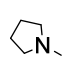
**Scheme 1.** Synthesis of **4a**-**4d**[a]



4a: R$_1$=

4b: R$_1$=

4c: R$_1$=

4d: R$_1$=

[a]Reagents and conditions: (a) ethyl 2-(diethoxyphosphoryl) acetate, K$_2$CO$_3$, EtOH, 100°C; (b) **4a**-**4b**: K$_2$CO$_3$, Pd(PPh$_3$)$_4$, 1,4-dioxane, 100°C; **4c**-**4d**: Pd(dba)$_3$, CsCO$_3$, 4,5-Bis(diphenylphosphino)-9,9-dimethylxanthene, 1,4-dioxane, 100°C.

**Scheme 2.** Synthesis of **8a**-**8f**[a]



[a]Reagents and conditions: (c) MCPBA, $K_2CO_3$, DCM, r.t.; (d) NaOH (1N), 60°C; (e) *N,N'*-Carbonyldiimidazole, THF, r.t.; (f) **8a**-**8c**: $K_2CO_3$, Pd(PPh$_3$)$_4$, 1,4-dioxane, 100°C; **8d**-**8f**: Pd(OAc)$_2$, Tri(o-tolyl)phosphine, Et$_3$N, DMF, 100°C.

**Scheme 3.** Synthesis of **10a**-**10e**[a]
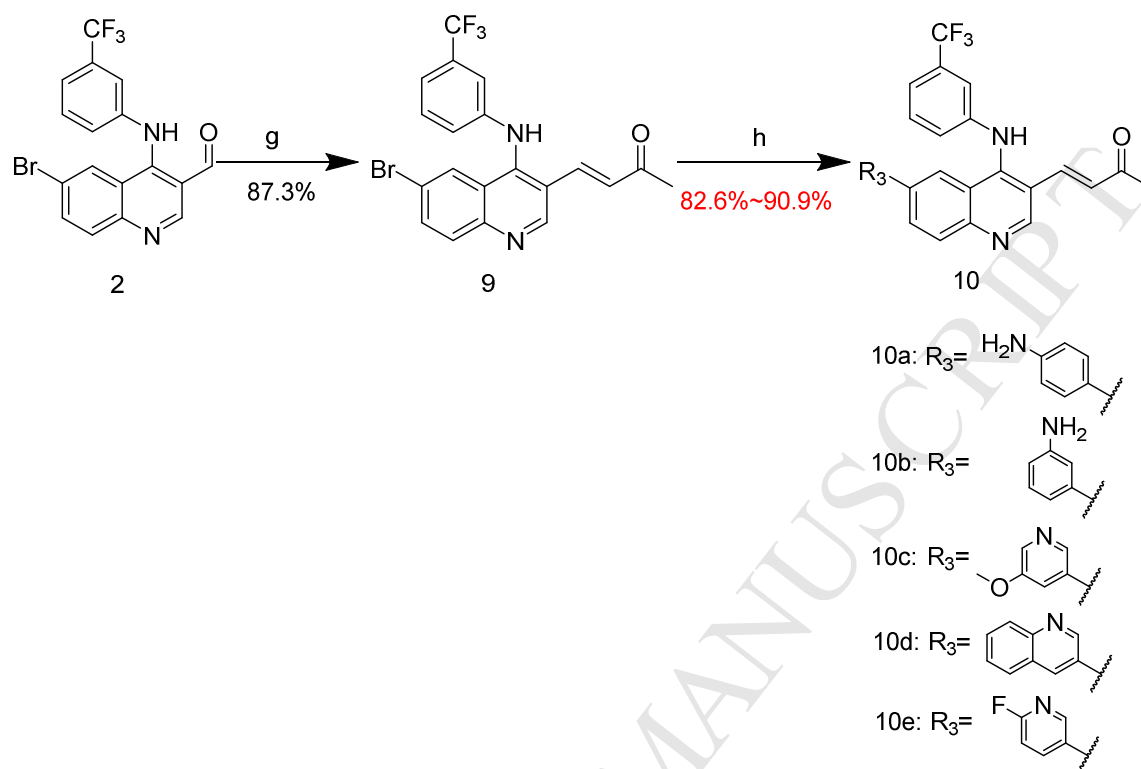


[a]Reagents and conditions: (g) 1-(triphenylphosphoranylidene)propan-2-one, DMSO, 120°C; (h) $K_2CO_3$, Pd(PPh$_3$)$_4$, 1,4-dioxane, 100°C.

**Scheme 4.** Synthesis of **11a**-**11o**[a]



11a:$R_4$=F;$R_5$=$R_6$=H

11b:$R_6$=F;$R_4$=$R_5$=H

11c:$R_4$=$OCH_3$;$R_5$=$R_6$=H

11d:$R_6$=$OCH_3$;$R_4$=$R_5$=H

11e:$R_6$=$CH_3CH_2(CO)NH$;$R_4$=$R_5$=H

11f:$R_6$=$CH_3(CH_2)_2(CO)NH$;$R_4$=$R_5$=H

11g:$R_6$=$(CH_3)_2CH(CO)NH$;$R_4$=$R_5$=H

11h:$R_6$=$CH_3(CH_2)_3(CO)NH$;$R_4$=$R_5$=H

11i:$R_6$=$C_6H_5CH_2(CO)NH$;$R_4$=$R_5$=H

11j:$R_6$=$(CH_3)_3CO(CO)NH$;$R_4$=$R_5$=H

11k:$R_6$=$C_6H_5OOCNH$;$R_4$=$R_5$=H

11l:$R_6$=$C_6H_5CH_2OOCNH$;$R_4$=$R_5$=H

11m:$R_6$= [structure] $R_4$=$R_5$=H

11n:$R_6$= [structure] $R_4$=$R_5$=H

11o:$R_6$= [structure] $R_4$=$R_5$=H

[a]Reagents and conditions: (i) $K_2CO_3$, $Pd(PPh_3)_4$, 1,4-dioxane, 100°C.

40

Highlights

- Synthesis of novel Compd targeting mTOR for anti-EV71.
- Preliminary explore the new mechanism of anti-EV71 based on mTOR.